Alexander Meeh, BSc

Space-Time Methods for the One Dimensional Wave Equation

MASTER'S THESIS

to obtain the academic degree

Diplom-Ingenieur

Master's degree programme - Civil Engineering and Structural Engineering

submitted to

Graz University of Technology

Supervisor
Univ.-Prof. Dr.-Ing. Martin Schanz

Institute of Applied Mechanics

Supervising assistant
Dipl.-Ing. Dominik Pölz

Graz, August 2018

Statutory Declaration

I declare that I have authored this thesis independently, that I have not used other than the declared sources/resources, and that I have explicitly indicated all material which has been quoted either literally or by content from the sources used. The text document uploaded to TUGRAZonline is identical to the present master‘s thesis.

Date	Signature

Eidesstattliche Erklärung

Ich erkläre an Eides statt, dass ich die vorliegende Arbeit selbstständig verfasst, andere als die angegebenen Quellen/Hilfsmittel nicht benutzt, und die den benutzten Quellen wörtlich und inhaltlich entnommenen Stellen als solche kenntlich gemacht habe. Das in TUGRAZonline hochgeladene Textdokumentist mit der vorliegenden Masterarbeit identisch.

Datum	Unterschrift

Abstract

This work covers space-time finite element methods. Two dynamic problems which are closely related to each other are presented. In particular, the wave equation for the elastic bar and the acoustic fluid in the one dimensional case are discussed. Therefore, we give a derivation of the mechanical problems and formulate a variational problem for each initial boundary value problem. A Bubnov Galerkin method for the elastic bar and a discontinuous Petrov Galerkin method for the acoustic fluid are presented. Both methods are formulated in the space-time setting. The variational problems are transferred to a discrete setting in which standard finite element technology is utilised for an entire initial boundary value problem. Finally, a verification of the proposed space-time methods is done by a numerical approach and several examples are investigated.

Zusammenfassung

In dieser Arbeit werden Raum-Zeit Finite Elemente Methoden behandelt. Dazu werden zwei dynamische Probleme hergeleitet und vorgestellt. Im Speziellen handelt es sich hierbei um den elastischen Dehnstab und das akustische Fluid im ein-dimensionalen Fall. Beide mechanische Probleme werden durch die Wellengleichung beschrieben. Es wird für das Problem des Dehnstabs, sowie des Fluids jeweils eine Variationsformulierung vorgestellt. Ein Bubnov-Galerkin Verfharen wird für den elastischen Dehnstab und ein diskontinuierliches Petrov-Galerkin Verfahren für das akustische Fluid behandelt. Beide Methoden werden in Raum-Zeit formuliert, um eine gewöhnliche Finite Elemente Technologie für das gesamte Anfangsrandwertproblem anzuwenden. Schließlich werden die Raum-Zeit Methoden durch einen numerischen Ansatz verifiziert und es werden mehrere numerische Beispiele untersucht.

CONTENTS

1 INTRODUCTION

Time dependent problems arise in many engineering applications such as fluid dynamics, structural dynamics or signal processing. One can investigate such problems in the time or frequency domain. While treating such problems in the frequency domain is useful for harmonic excitations, time domain methods play an important role for problems with transient dynamic repsones. Within this work we focus on transient problems, in particular we restrict ourselves to the wave equation in the one dimensional case. Here, two physical problems are investigated, on the one hand the wave equation for the elastic bar and on the other hand for acoustic fluids. Their governing equations are derived from the fundamental theory of continuum mechanics. There are several textbooks on the topic of continuum mechanics such as [3, 27, 31]. There are analytical solutions available for the wave equation with special initial and boundary conditions. However, this is not the case in general. Therefore, one resorts to numerical solution techniques. Common methods are the finite difference method (FDM), finite element method (FEM) or boundary element method (BEM). The method of choice in this line of work is the FEM. For introductory information on this topic see, e.g. [11,18,24,34,36]. The finite element method makes use of a variational formulation of the governing equation. For time dependent problems it is standard practise to use a semi discretization where space and time are meshed independently. One approach is the method of lines [33], where first a discretization is deployed spatially and afterwards in time. After discretizing the spatial problem with a method of choice such as FEM one obtains a system of ordinary differential equations with respect to time which can be solved with classical finite differences such as forward/central/backward differences. Furthermore, there is Rothe's method [32], which discretizes in time first and afterwards in space leading to a system of stationary problems which is in general a system of partial differential equations and can be solved with the same set of methods. However, here, we use space-time methods which regard the time variable as an additional coordinate. Therefore, in contrast to above mentioned methods a discretization of the entire space-time domain is conducted. To illustrate this, a comparision of an approximation via a classic approach and a space-time approach is made. As seen in Figure 1.1a common approaches use only a spatial discretization which calculates a spatial solution at certain time positions only. In contrast to this, we observe a complete discretization of the space-time slab in 1.1b and, hence, obtain a solution everywhere in the space-time domain directly. Although space-time methods exist already for a longer period (*cf.* [22,23]), they were not commonly utilised until recently. Due to increasing computing performance space-time methods attract more attention recently. A big advantage of space-time methods is the ability to consider moving boundaries directly, since they grant direct acces to the defomerd configuration at all times. Furthermore, one can benefit from the ability

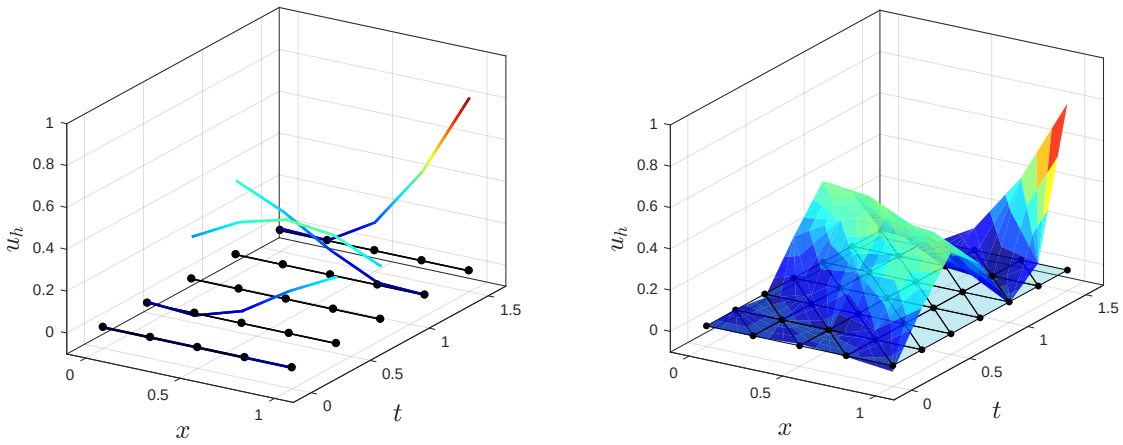

(a) Classic approach

(b) Space-time approach

Figure 1.1: Approximated solution $u_h(x,t)$ for a problem in dynamics

to refine a given mesh locally. This is of advantage when resolving local features of the analytical solution in space and time. Known adaptive space-time methods can be found in [1, 15, 30, 35].

In this work we will present two space-time methods. First, we will develop a Bubnov Galerkin method [28], which is a continuous Galerkin (CG) method for the wave equation of the elastic bar. The derived formulation has only the primal variable as its unknown, i.e. the displacement field. The initial and boundary conditions are imposed via the penalty method [7, 8] and the discretization is done with the use of the Argyris element [17]. Furthermore, we present a discontinuous Petrov Galerkin method (*cf.* [13, 14, 16]) for the first order system of the wave equation in acoustics according to [20]. Here, the pressure and velocity field are the unknowns. In a Petrov Galerkin formulation the test space differs from the trial space see, e.g. [6]. The central idea of the discontinuous Petrov Galerkin (DPG) method is to approximate the optimal test functions for a given trial space. This can be done locally, since a discontinuous formulations is used. For reference of classical discontinous Galerkin (DG) methods see, e.g. [5]. Furthermore, the DPG method has a built-in error estimator which allows for automatic adaptive refinement schemes. The discretization uses polynomial finite elements of Lagrangian type for the trial spaces and the test space. For a more comprehensive description of the Galerkin method the reader is referred to [28].

1.1 Outline

First, the mechanical problem setting is introduced in Chapter 2. Here, all governing equations for one dimensional dynamics are derived from the theory of continuum mechanics and two initial boundary value problems are constructed. In Chapter 3, a continuous variational formulation is obtained for the wave equation of the elastic bar and a discontinuous variational formulation for the wave equation of the acoustic fluid is presented. This is followed by Chapter 4 which deals with discretization techniques and brings both variational problems to a discrete setting resulting in a CG method for the elastic bar and a DPG method for the acoustic fluid. Furthermore, a short introduction in finite element spaces is given. Applications of the introduced space-time methods are given in Chapter 5. First, a verification example where convergence studies are conducted is investigated for both methods. Afterwards, we present a model problem showcasing typical features of the respective space-time methods and discussing its advantages and disadvantages. In the last chapter, a short conclusion is given.

2 MECHANICAL PROBLEM SETTING

In this chapter, two mechanical problems are discussed. In particular the dynamic behaviour of an elastic bar and of an acoustic fluid are investigated. In both cases, only geometries where one dimension is predominating are considered. This leads to the one dimensional wave equation for the solid and the fluid. We assume small changes of the state variables, such as the pressure field of the acoustic fluid and the displacement field of the elastic bar. This means higher order terms in the kinematic relations can be neglected. Furthermore, only linear constitutive models are considered. Due to these assumptions linear partial differential equations for both described cases are obtained.

2.1 Wave Equation for the Elastic Bar

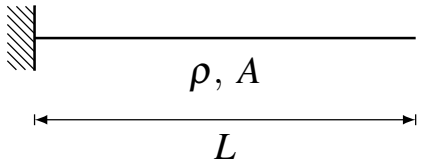

Figure 2.1: Elastic bar

This section deals with the derivation of the wave equation for the elastic bar. A bar is body where one of its dimensions is significantly larger than the others. Therefore, all relevant mechanical quantities of the bar can be described as functions along its axis. In particular a bar is defined between 0 and L where $L > 0$ is the length of the bar. Furthermore, it has a cross section area $A > 0$ and a density $\rho > 0$. These physical quantities define the mass $m = \rho AL$ of the bar. A bar has to have at least one support to be fixed in location and can be loaded by axial forces. Exemplary a bar which is fixed on the left side and is not supported on the right side is depicted in Figure 2.1. Here, only homogeneous and isotropic materials are considered. We call the displacement field of the elastic bar $u(x,t)$.

2.1.1 Kinematics

The relation between the deformation $u(x,t)$ and the strain $\varepsilon(x,t)$ is described by the kinematic relations. In Figure 2.2 the kinematic relation for a deformed infinitesimal bar ele-

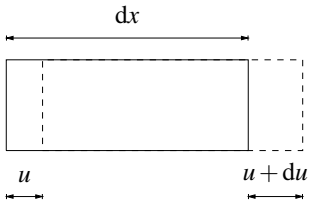

Figure 2.2: Deformed infinitesimal bar element

ment is illustrated. This leads to the relation of the infinitesimal strain for the one dimensional case. It reads

$$\varepsilon = \frac{u + \mathrm{d}u - u}{\mathrm{d}x} = \partial_x u. \tag{2.1}$$

2.1.2 Balance Laws and Kinetics

Independent of the material properties for a given physical object, there are relations between the external loading and the internal response which are expressed by the kinetics of the given body. Thus, the kinetic relations hold for every solid or fluid. Within this work only mechanical loadings are considered. We distinguish between body forces $f(x,t)$ which act on the whole body and traction forces $q(t)$ which act only on the boundary of the body. The external forces produce internal forces which can be described by the stress state $\sigma(x,t)$. In the one dimensional case only stresses in x-direction appear. We define the internal normal force $N(x,t)$ with

$$N = \int_A \sigma \, \mathrm{d}A. \tag{2.2}$$

At an infinitesimal bar element as depicted in Figure 2.3 one can observe the kinetic equilibrium which results in the balance of linear momentum or equilibrium of forces

$$\mathrm{d}m \partial_{tt} u = N + \mathrm{d}N - N + fA \, \mathrm{d}x, \tag{2.3}$$

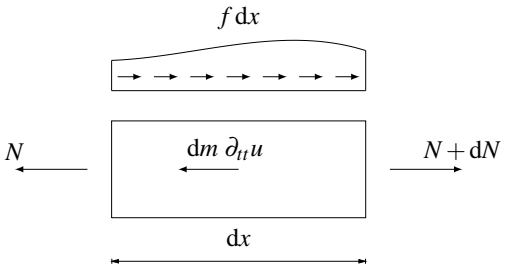

Figure 2.3: Free body diagram

with $\mathrm{d}m = \rho A \,\mathrm{d}x$. This equation is rewritten as

$$\rho A \partial_{tt} u = \partial_x N + fA. \tag{2.4}$$

2.1.3 Constitutive Relations

The constitutive model connects kinematics and kinetics and thus a relation between $\sigma(x,t)$ and $\varepsilon(x,t)$. As stated above only homogeneous and isotropic materials are considered. Here, we use the Kelvin-Voigt model whose rheological model connects a spring element and a dash pot in parallel. It reads

$$\sigma = E\varepsilon + D\partial_t \varepsilon, \tag{2.5}$$

where $E > 0$ is the Young's modulus and $D > 0$ the viscosity. For further information on this topic the reader is referred to [12].

2.1.4 Initial Boundary Value Problem

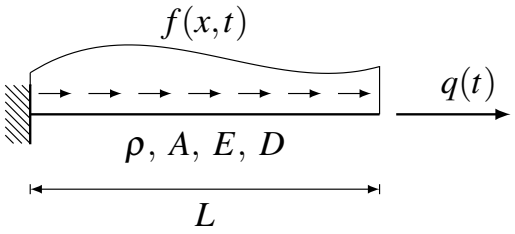

Figure 2.4: Elastic bar under load

Before we construct the initial boundary value problem we derive the governing equation for this problem. Exemplary, an elastic bar which is fixed on the left side and subjected to a time dependent traction force $q(t)$ and an axial body force $f(x,t)$, is depicted in Figure 2.4. Combining relation (2.1), (2.4) and (2.5) results in the following governing equation for the damped axial vibration

$$\partial_{tt} u - c^2 \partial_{xx} u - d^2 \partial_{xxt} u = \frac{f}{\rho}, \tag{2.6}$$

where $c^2 = E/\rho$, $d^2 = D/\rho$. In order to define an initial boundary value problem we introduce the space-time domain Q which is constructed as follows. We consider a time interval $\Upsilon = (0,T)$ where $T > 0$ is an arbitrary end time and a space domain or spatial interval $\Omega = (0,L)$. Furthermore, we introduce the boundary Γ of the space domain defined

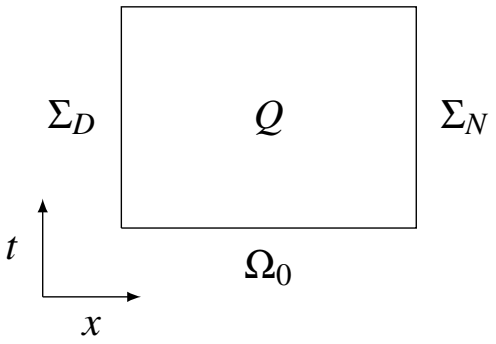

Figure 2.5: The space-time domain for the elastic bar element

by $\Gamma = \partial\Omega = \{0, L\}$. The boundary can be decomposed as follows $\Gamma = \Gamma_D \cup \Gamma_N$ while Γ_D defines the Dirichlet boundary of the domain Ω relating to displacement boundary conditions and Γ_N defines a Neumann type boundary of Ω relating to boundary conditions which impose traction forces. Thus, the space-time domain is defined by $Q = \Omega \times \Upsilon$ with its lateral boundary denoted by $\Sigma = \Gamma \times \Upsilon$ with $\Sigma_D = \Gamma_D \times \Upsilon$, $\Sigma_N = \Gamma_N \times \Upsilon$ and its initial boundary $\Omega_0 = \Omega \times \{t = 0\}$. The graphical representation of this setting is depicted in Figure 2.5. Thus, the initial-boundary value problem for the elastic bar element reads

$$\partial_{tt} u - c^2 \partial_{xx} u - d^2 \partial_{xxt} u = \frac{f}{\rho} \quad \text{in } Q$$

$$\begin{aligned} u &= u_0 && \text{on } \Omega_0 \\ \partial_t u &= \dot{u}_0 && \text{on } \Omega_0 \\ u &= \tilde{u} && \text{on } \Sigma_D \\ c^2 \partial_x u + d^2 \partial_{xt} u &= \frac{q}{\rho A} && \text{on } \Sigma_N. \end{aligned} \tag{2.7}$$

2.2 Wave Equation for the Acoustic Fluid

In this section, we derive the first order system of the wave equation for acoustic fluids. This can be done in different ways, for a more comprehensive derivation see [19, 29]. A fluid is called acoustic fluid if it is homogeneous, isotropic, perfectly elastic and at rest in the initial state. With these restrictions we denote the total density $\hat{\rho}(x,t)$ and pressure field $\hat{p}(x,t)$. Furthermore, the states at rest of the density and pressure are denoted by ρ_0

and p_0. Hence, the density and pressure field are decomposed as follows

$$\hat{\rho}(x,t) = \rho(x,t) + \rho_0,$$
$$\hat{p}(x,t) = p(x,t) + p_0.$$

In the following only small fluctuations of the density $\rho \ll \rho_0$ and the pressure $p \ll p_0$ are considered. Note that $v(x,t) = \partial_t u(x,t)$.

2.2.1 Kinematics

The volume change, also known as dilatation $\varepsilon(x,t)$ can be written as

$$\varepsilon = \frac{\mathrm{d}V - \mathrm{d}V_0}{\mathrm{d}V_0}, \tag{2.8}$$

where V denotes the volume at a certain point (x,t) and V_0 the initial volume at position x. Since it holds $\hat{\rho}(x,t)\,\mathrm{d}V(x,t) = \rho_0\,\mathrm{d}V_0(x)$, we rewrite the kinematic relation (2.8) with

$$\rho = -\hat{\rho}\varepsilon. \tag{2.9}$$

Assuming that the fluctuations are sufficiently small, we can linearize (2.9) which results in

$$\rho = -\rho_0\varepsilon. \tag{2.10}$$

2.2.2 Balance Laws and Kinetics

In the case of acoustic fluids the balance of mass and balance of linear momentum are observed. The balance of mass is given with

$$\partial_t\hat{\rho} + \partial_x(\hat{\rho}v) = g, \tag{2.11}$$

where $g(x,t)$ is a mass source. Only small fluctuations and homogeneous fluids are assumed, hence (2.11) can be linearised and we obtain

$$\partial_t\rho + \rho_0\partial_x v = g. \tag{2.12}$$

In an acoustic fluid the stress tensor is hydrostatic. This means in the three dimensional space $\sigma(x,t) = -p(x,t)\,\mathrm{I}$, where I denotes the identity matrix. In the one dimensional case this relation reads

$$\sigma = -p. \tag{2.13}$$

Consequently, with (2.13) the balance of linear momentum in the one dimensional case is obtained

$$\rho_0\partial_t v - \partial_x p = f. \tag{2.14}$$

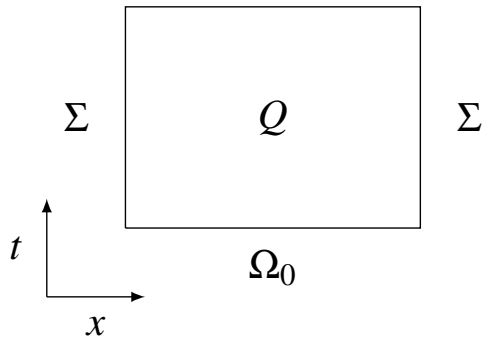

Figure 2.6: The space-time domain for the acoustic fluid

2.2.3 Constitutive Relations

The constitutive relation of an acoustic fluid is given with a relation between the density $\rho(x,t)$ and the pressure $p(x,t)$. In particular, it reads

$$p = -K\varepsilon, \tag{2.15}$$

with the bulk modulus $K > 0$.

2.2.4 Initial Boundary Value Problem

We obtain the governing system of equations by combining (2.10), (2.12), (2.14) and (2.15) which results in

$$\begin{aligned} \partial_t v - \frac{1}{\rho_0}\partial_x p &= \frac{f}{\rho_0}, \\ \frac{1}{K}\partial_t p - \partial_x v &= \frac{g}{\rho_0}. \end{aligned} \tag{2.16}$$

We construct a similar space-time domain Q as shown in Section 2.1.4. We consider the same spatial interval Ω and time intervals Υ such that $Q = \Omega \times \Upsilon$ where $\Omega_0 = \Omega \times \{t = 0\}$, with the initial conditions for the pressure and velocity. However, we only consider boundary conditions for the pressure field which are given on $\Sigma = \{0, L\} \times \Upsilon$. Thus, the

initial-boundary value problem for the acoustic fluid reads

$$\begin{aligned} \rho_0 \partial_t v - \partial_x p &= f && \text{in } Q \\ \frac{1}{K} \partial_t p - \partial_x v &= \frac{g}{\rho_0} && \text{in } Q \end{aligned} \tag{2.17}$$

$$\begin{aligned} p &= p_0 && \text{on } \Omega_0 \\ v &= v_0 && \text{on } \Omega_0 \\ p &= \tilde{p} && \text{on } \Sigma. \end{aligned}$$

2.3 Comparison of the Elastic Bar and the Acoustic Fluid

Both presented mechanical problems correlate to each other since the first order system of the wave equation can be transformed in a second order wave equation which relates to (2.6). This can be done for both variables $v(x,t)$ and $p(x,t)$. We assume that the source term $g(x,t)$ vanishes. We start with deriving the second order wave equation for the pressure field $p(x,t)$. The first equation of (2.16) is differentiated with respect to x while the second equation is differentiated with respect to t. Lastly, both equations are inserted into each other leading to

$$\frac{\rho_0}{K} \partial_{tt} p - \partial_{xx} p = \partial_x f, \tag{2.18}$$

for $(x,t) \in Q$. For velocity $v(x,t)$ we differentiate the first equation of (2.16) with respect to t and the second equation with respect to x and obtain

$$\rho_0 \partial_{tt} v - K \partial_{xx} v = \partial_t f, \tag{2.19}$$

for $(x,t) \in Q$. Lastly by integrating (2.19) with respect to time one obtains

$$\rho_0 \partial_{tt} u - K \partial_{xx} u = f + C, \tag{2.20}$$

for $(x,t) \in Q$ and where C is some constant which is zero for suitable boundary conditions. At this point, one can observe the direct connection between both mechanical problem settings.

3 VARIATIONAL FORMULATIONS

In the course of this chapter, a variational formulation of the wave equation for the elastic bar and of the wave equation for the acoustic fluid is derived. In the case of the elastic bar we obtain a weak formulation with respect to space. However, the variational formulation is kept in a strong form with respect to time. Due to this fact, this method requires sufficiently smooth functions.

For the acoustic fluid the space-time domain is decomposed and a variational formulation which allows discontinuities between the partitions is presented. This results in a mesh dependent variational formulation which is a typical feature of DG methods. The obtained formulation is also called a broken weak formulation. The DPG method which calculates the test space according to the trial space is built on this formulation. From here on, we use the notation u for trial functions and v for test functions.

3.1 CG Formulation for the Elastic Bar

In order to solve (2.7) we reformulate it in a weak sense. To this end, we multiply (2.6) with the time derivative of the test function v and apply integration by parts with respect to space. This leads to the problem: Find $u(x,t) \in U$ such that

$$\int_Q \partial_{tt} u \partial_t v \,\mathrm{d}Q + \int_Q \left(c^2 \partial_x u + d^2 \partial_{xt} u\right) \partial_{xt} v \,\mathrm{d}Q - \int_\Sigma \left(c^2 \partial_x u + d^2 \partial_{xt} u\right) \partial_t v \,\mathrm{d}\Sigma = \int_Q \frac{f}{\rho} \partial_t v \,\mathrm{d}Q \quad (3.1)$$

holds for all $v(x,t) \in U$, where U is a suitable space. Note that within this work the well-posedness of this variational formulation is not further investigated and is still an open question. In particular, we assume that all partial derivatives in (3.1) are in $L_2(Q)$. To avoid restrictions for the space U when imposing initial and Dirichlet boundary conditions, a penalty method [7, 8] is applied. Therefore, the exact Dirichlet boundary condition

$$u - \tilde{u} = 0, \quad (3.2)$$

on Σ_D is replaced by an approximate condition

$$u - \tilde{u} + \gamma_B \left(c^2 \partial_x u + d^2 \partial_{xt} u\right) = 0, \quad (3.3)$$

where $\gamma_B > 0$ is the penalty parameter. In order that (3.3) approximates the the boundary condition (3.2) good enough γ_B must be chosen sufficiently small. By multiplying (3.3) with the time derivative of the test function and integration over Σ we get

$$\int_{\Sigma} \left(c^2 \partial_x u + d^2 \partial_{xt} u \right) \partial_t v \, \mathrm{d}\Sigma = \int_{\Sigma_N} \frac{q}{\rho A} \partial_t v \, \mathrm{d}\Sigma_N - \frac{1}{\gamma_B} \int_{\Sigma_D} (u - \tilde{u}) \partial_t v \, \mathrm{d}\Sigma_D. \tag{3.4}$$

Analogously, a penalty term for the initial conditions

$$\begin{aligned} u - u_0 &= 0, \\ \partial_t u - \dot{u}_0 &= 0 \end{aligned} \tag{3.5}$$

is formulated. These conditions are, then, imposed by adding following integral

$$\begin{aligned} u - u_0 &= \frac{1}{\gamma_B} \int_{\Omega_0} (u - u_0) \partial_t v \, \mathrm{d}\Omega_0, \\ \partial u - \dot{u}_0 &= \frac{1}{\gamma_B} \int_{\Omega_0} (\partial_t u - \dot{u}_0) \partial_t v \, \mathrm{d}\Omega_0 \end{aligned} \tag{3.6}$$

to (3.1). The combination of (3.1), (3.4), and (3.6) gives the penalized variational formulation to be solved. For further explanations we introduce the bilinear form $b(u,v)$ and the linear form $\ell(v)$ defined as

$$\begin{aligned} b(u,v) = &\int_{Q} \left(\partial_{tt} u \partial_t v + c^2 \partial_x u \partial_{xt} v + d^2 \partial_{xt} u \partial_{xt} v \right) \mathrm{d}Q \\ &+ \frac{1}{\gamma_B} \left[\int_{\Sigma_D} u \partial_t v \, \mathrm{d}\Sigma_D + \int_{\Omega_0} (u \partial_t v + \partial_t u \partial_t v) \, \mathrm{d}\Omega_0 \right], \\ \ell(v) = &\int_{Q} \frac{f}{\rho} \partial_t v \, \mathrm{d}Q + \int_{\Sigma_N} \frac{q}{\rho A} \partial_t v \, \mathrm{d}\Sigma_N + \frac{1}{\gamma_B} \left[\int_{\Sigma_D} \tilde{u} \partial_t v \, \mathrm{d}\Sigma_D + \int_{\Omega_0} (u_0 \partial_t v + \dot{u}_0 \partial_t v) \, \mathrm{d}\Omega_0 \right]. \end{aligned} \tag{3.7}$$

Then, the problem reads: Find $u \in U$ such that

$$b(u,v) = \ell(v) \tag{3.8}$$

holds for all test functions $v \in U$. The realisation of this method is given in Chapter 4, where this problem is formulated in a discrete setting.

3.2 DPG Formulation for the Acoustic Fluid

The variational formulation for the acoustic fluid is derived according to [20]. That is why the function spaces are defined more rigorously. In this setting we use a notation where the physical meaning of the state variables is represented via subscripts. In particular u_v for v and u_p for p. Thus, we partition the trial function u block wise leading to

$$u = \begin{bmatrix} u_v \\ u_p \end{bmatrix}, \tag{3.9}$$

where $u_v, u_p \in L_2(Q)$ and consequently $u \in L_2(Q)^2$. We introduce a wave operator $\mathrm{A} : W(Q) \to L_2(Q)^2$ with

$$\mathrm{A}\,u = \begin{bmatrix} \rho_0 \partial_t u_v - \partial_x u_p \\ \frac{1}{K}\partial_t u_p - \partial_x u_v \end{bmatrix}, \tag{3.10}$$

where $W(Q)$ is defined by

$$W(Q) = \{u \in L_2(Q)^2 : \mathrm{A}\,u \in L_2(Q)^2\}. \tag{3.11}$$

With the scalar product $(u,v)_{L_2(Q)^2} = \int_Q u \cdot v \,\mathrm{d}Q$ from Appendix A $(\mathrm{A}\,u, v)_{L_2(Q)^2}$ is given with

$$(\mathrm{A}\,u, v)_{L_2(Q)^2} = \int_Q \begin{bmatrix} \rho_0 \partial_t u_v - \partial_x u_p \\ \frac{1}{K}\partial_t u_p - \partial_x u_v \end{bmatrix} \cdot \begin{bmatrix} v_v \\ v_p \end{bmatrix} \mathrm{d}Q. \tag{3.12}$$

For sufficiently smooth functions we apply integration by parts on (3.12) and obtain

$$\begin{aligned}(\mathrm{A}\,u, v)_{L_2(Q)^2} = \rho_0 \int_{\partial Q} u_v v_v n_t \,\mathrm{d}\partial Q - \int_{\partial Q} u_p v_v n_x \,\mathrm{d}\partial Q + \frac{1}{K}\int_{\partial Q} u_p v_p n_t \,\mathrm{d}\partial Q - \int_{\partial Q} u_v v_p n_x \,\mathrm{d}\partial Q \\ - \rho_0 \int_Q u_v \partial_t v_v \,\mathrm{d}Q + \int_Q u_p \partial_x v_v \,\mathrm{d}Q - \frac{1}{K}\int_Q u_p \partial_t v_p \,\mathrm{d}Q + \int_Q u_v \partial_x v_p \,\mathrm{d}Q.\end{aligned} \tag{3.13}$$

The boundary term of (3.13) induces the operator $\mathrm{D} : W \to W^*$ and is for sufficiently smooth functions u, v represented by

$$(\mathrm{D}\,u)(v) = \int_{\partial Q} \left[u_v(\rho_0 n_t v_v - n_x v_p) + u_p(-n_x v_v + \frac{1}{K} n_t v_p) \right] \mathrm{d}\partial Q, \tag{3.14}$$

where n denotes the unit normal vector (n_x, n_t) of Q. Furthermore, one can observe that the volumetric term of (3.13) is the application of A on the second argument in the inner product. This leads to the reformulation of (3.14) as follows

$$\langle \mathrm{D}\,u, v \rangle_W \coloneqq (\mathrm{D}\,u)(v) = (\mathrm{A}\,u, v)_{L_2(Q)^2} + (u, \mathrm{A}\,v)_{L_2(Q)^2}, \tag{3.15}$$

where $\langle \cdot, \cdot \rangle_W$ denotes the duality pairing in W. In order to arrive at the variational formulation the trial space for given space time domain Q will be broken. Therefore, a decomposition of the space-time domain $Q_h = Q$ is obtained defined by

$$\overline{Q_h} = \bigcup_{\tau \in Q_h} \overline{\tau}, \tag{3.16}$$

where τ is an open subset of Q and h relates to the size of the subset. For a more comprehensive definition see Chapter 4 where the details of discretization techniques are covered and h and τ are introduced properly. We define the piecewise wave operator A_h by

$$(\mathrm{A}_h w)|_\tau = \mathrm{A}(w|_\tau), \tag{3.17}$$

for $w \in W(\tau)$. In a way, A_h represents the piecewise application of A with respect to the decomposition which means the governing equation must only hold on element level. We define

$$W_h = \{w \in L_2(Q)^2 : \mathrm{A}_h w \in L_2(Q)^2\}. \tag{3.18}$$

Analogously the operator $\mathrm{D}_h : W_h \to W_h^*$ is introduced for which holds

$$\langle \mathrm{D}_h w, v \rangle_{W_h} = (\mathrm{A}_h w, v)_{L_2(Q)^2} + (w, \mathrm{A}_h v)_{L_2(Q)^2}. \tag{3.19}$$

for all $w, v \in W_h$.

We introduce the space $R := \mathrm{D}_h(V)$ where $V \subset W(Q)$ is a Hilbert space. For details on V see [20]. Then, the bilinear form reads

$$b((u,r),w) = -(u, \mathrm{A}_h w)_{L_2(Q)^2} + \langle r, w \rangle_{W_h}, \tag{3.20}$$

where $(u,r) \in L_2(Q)^2 \times R$ and $w \in W_h$. Then, the variational problem is formulated: Find $u \in U = L_2(Q)^2$ and $r \in R$ such that

$$b((u,r),w) = \ell(w) \tag{3.21}$$

holds for all $w \in W_h$.

Note that the wellposedness of this formulation is established, the proof for this can be found in [20]. The ideal DPG method uses the trial to test operator $\mathrm{T} : U \times R \to W_h$ to construct optimal test functions from trial functions. For each $(u,r) \in U \times R$ define $\mathrm{T}(u,r)$ by

$$(\mathrm{T}(u,r), w)_{W_h} = b((u,r),w) \qquad \forall w \in W_h. \tag{3.22}$$

This operator is well-defined by the Riesz representation theorem (Theorem A.1). The given trial to test operator T allows for the calculation of optimal test functions. We show in the following that $w = \mathrm{T}(u,r)$ realises the supremum in the inf-sup condition. It holds

$$\sup_{w\in W_h\setminus\{0\}} \frac{b((u,r),w)}{\|w\|_{W_h}} = \sup_{w\in W_h\setminus\{0\}} \frac{(\mathrm{T}(u,r),w)_{W_h}}{\|w\|_{W_h}}, \tag{3.23}$$

and with $w = \mathrm{T}(u,r)$ we obtain directly

$$\sup_{w\in W_h\setminus\{0\}} \frac{(\mathrm{T}(u,r),w)_{W_h}}{\|w\|_{W_h}} \geq \frac{(\mathrm{T}(u,r),\mathrm{T}(u,r))_{W_h}}{\|\mathrm{T}(u,r)\|_{W_h}} = \|\mathrm{T}(u,r)\|_{W_h}. \tag{3.24}$$

Furthermore, we use the Cauchy-Schwarz inequality (A.1) to arrive at

$$\sup_{w\in W_h\setminus\{0\}} \frac{(\mathrm{T}(u,r),w)_{W_h}}{\|w\|_{W_h}} \leq \sup_{w\in W_h\setminus\{0\}} \frac{\|\mathrm{T}(u,r)\|_{W_h}\|w\|_{W_h}}{\|w\|_{W_h}} = \|\mathrm{T}(u,r)\|_{W_h}. \tag{3.25}$$

This means the supremum is a maximum and it holds

$$\|\mathrm{T}(u,r)\|_{W_h} = \sup_{w\in W_h\setminus\{0\}} \frac{(\mathrm{T}(u,r),w)_{W_h}}{\|w\|_{W_h}}. \tag{3.26}$$

Thus, the inf-sup condition translates directly onto the discretization when using the exact trial to test operator T. However, T is not known in a continuous setting. It has to be constructed in an approximate analogue leading to the discrete trial to test operator T_h. This is presented in Chapter 4.

4 DISCRETIZATION

After obtaining a variational formulation, a discretization of the given domain is constructed which means in particular, the variational problem is reformulated from an infinite dimensional space to a finite dimensional space. This form is also called discrete variational formulation. The finite dimensional spaces are also known as finite element spaces which span a subspace of the given infinite space. Thus, variational problems formulated on discrete spaces assemble systems of equations which are in this line of work sparse. For further information on discretization techniques the reader is referred to [11, 24, 34].

4.1 Triangulations

The space-time domain Q is discretized by a sequence of finite elements. In particular, a triangulation with N finite elements is defined by

$$\overline{Q} = \overline{\mathcal{T}}_N = \bigcup_{l=1}^{N} \overline{\tau}_l, \tag{4.1}$$

where τ_l denotes the l-th element of the discretization. In this line of work, only one dimensional mechanical problems are discussed. Therefore, the space-time domain of such a problem has an additional coordinate and, hence, is two dimensional, i.e. $Q \subset \mathbb{R}^2$. Furthermore, no moving boundaries are considered which means the space-time domain Q is a rectangle and consequently is displayed exactly. As geometric representation of the finite elements τ_l we use triangles. They are described by three nodes $\mathbf{x}_1^l, \mathbf{x}_2^l, \mathbf{x}_3^l$. The reference element $\hat{\tau}$ has the reference nodes $\hat{\mathbf{x}}_1 = (0,0),\ \hat{\mathbf{x}}_2 = (1,0),\ \hat{\mathbf{x}}_3 = (0,1)$. We

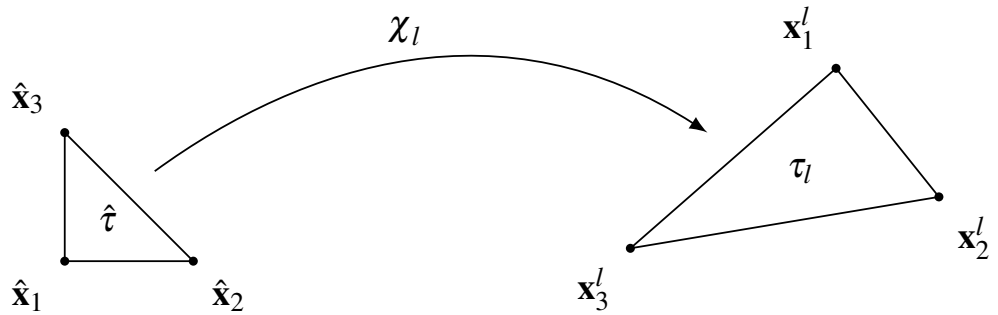

Figure 4.1: Affine mapping χ_l

introduce an affine mapping $\chi_l : \hat{\tau} \to \tau_l$ which maps from the reference triangle to the real triangle as depicted in Figure 4.1 and is given with

$$\mathbf{x} = \chi_l(\hat{\mathbf{x}}) = \mathrm{J}_l \hat{\mathbf{x}} + \mathbf{x}_1^l. \tag{4.2}$$

The matrix J_l denotes the Jacobi matrix of τ_l defined by

$$\mathrm{J}_l = \begin{bmatrix} x_2^l - x_1^l & x_3^l - x_1^l \\ t_2^l - t_1^l & t_3^l - t_1^l \end{bmatrix}. \tag{4.3}$$

This matrix is invertible and $\det \mathrm{J}_l$ is proportional to the area of τ_l, in particular

$$\Delta_l = \int_{\tau_l} \mathrm{d}\tau_l = \int_{\tau} |\det \mathrm{J}_l| \, \mathrm{d}\hat{\tau} = \frac{1}{2} |\det \mathrm{J}_l|, \tag{4.4}$$

We denote the size of τ_l by

$$h_l = \sqrt{\Delta_l}. \tag{4.5}$$

Furthermore, we introduce the global mesh parameter h with

$$h = \max_{\tau_l \in \mathcal{T}_N} h_l. \tag{4.6}$$

Exemplary, a uniform triangulation on the unit square is depicted in Figure 4.2.

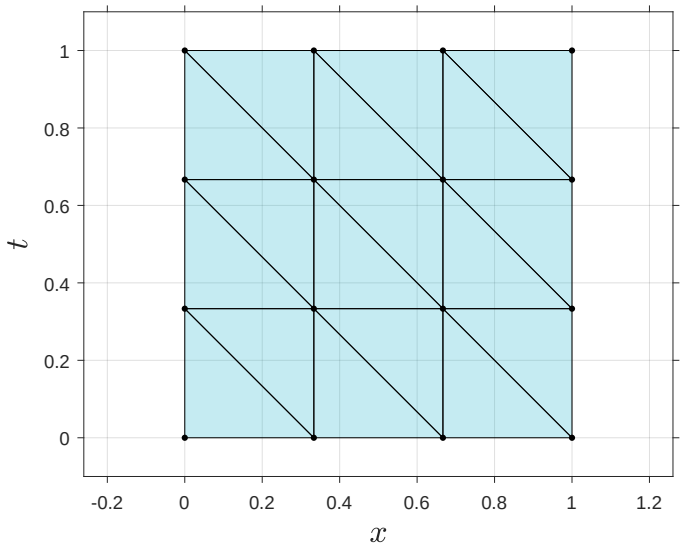

Figure 4.2: A standard triangulation $\mathcal{T}_{18}$

4.2 Finite Element Spaces

A finite element space approximates the infinite dimensional space from variational formulation. In this work we introduce three different finite element spaces also known as trial spaces. They are piecewise polynomial on the given triangulation and define the so called basis functions φ which are related to the M global degrees of freedom in the finite element space of a given triangulation $\mathcal{T}_N$. In particular, for a given space V it holds

$$V_h = \text{span}\{\varphi_i : i = 1, ..., M\} \subset V, \tag{4.7}$$

where V_h is a finite dimensional space which relates to V. The construction of the basis functions φ is done locally by means of the shape functions ψ. Therefore, the shape functions are defined element-wise, i.e. they are defined on the reference element $\hat{\tau}$ and transformed to a real element τ_l of a given triangulation. In particular, the shape functions for a Lagrangian space are defined by

$$\psi_i(\mathbf{x}_j) = \delta_{ij}, \tag{4.8}$$

where $\mathbf{x}_i$ denotes the i-th node of the triangle and δ_{ij} Kronecker delta defined by

$$\delta_{ij} = \begin{cases} 0 & \text{if } i \neq j, \\ 1 & \text{if } i = j. \end{cases} \tag{4.9}$$

Exemplary, the linear shape functions are illustrated in Figure 4.3. In Appendix B more information on the construction of the shape functions on the reference element is given. Consequently, one basis function φ_i is associated with a set of shape functions ψ_j, as illustrated in Figure 4.4. We remark that in case of linear shape functions, the nodes coincide

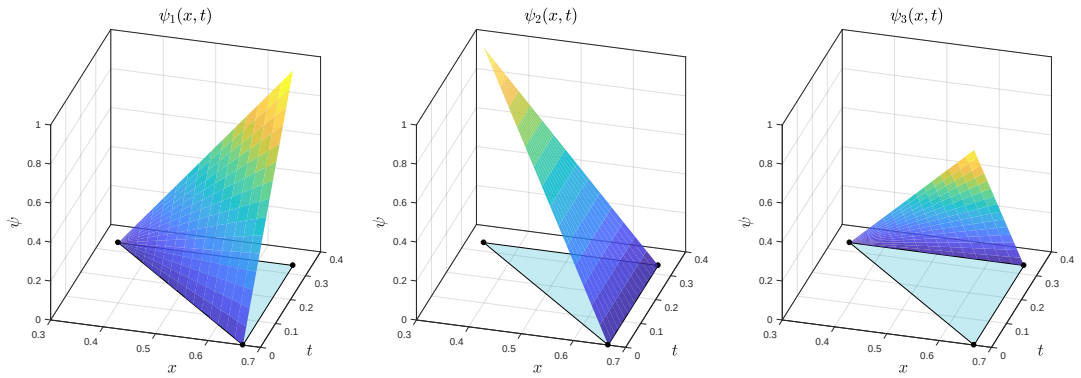

Figure 4.3: Linear Lagrange shape functions $\psi_j(x,t) \in \mathbb{P}^1(\tau_l)$

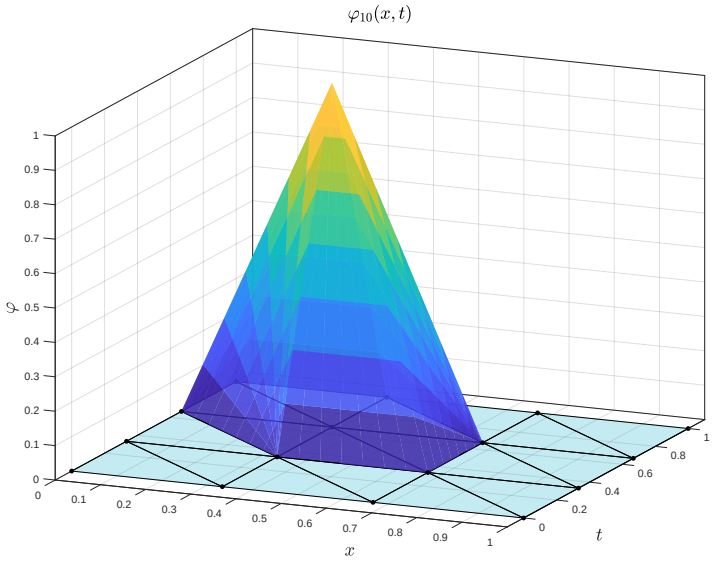

Figure 4.4: A linear basis function $\varphi(x,t)$ of the space $\mathcal{S}_h^{1,0}(\mathcal{T}_{18})$

with the vertices of the triangle. However, for shape functions with a higher polynomial degree additional nodes between the vertices and inside the element are necessary. For information on this topic see, e.g. [26]. With Lagrangian shape functions only a continuous function space can be constructed. In order to built spaces with higher continuity requirements one has to resort to other finite element spaces. In this line of work, we use the space of Argyris elements. The shape functions of the Argyris element also use the Kronecker delta property. However, they consider not only the nodal values but also their derivatives and the normal derivatives of the edges

$$\begin{aligned} \psi_i(\mathbf{x}_j) &= \delta_{ij}, \\ \partial_\circ \psi_i(\mathbf{x}_j) &= \delta_{ij}, \quad \circ \in \{x,t\} \\ \partial_\circ^2 \psi_i(\mathbf{x}_j) &= \delta_{ij}, \quad \circ \in \{xx,xt,tt\} \\ \nabla\psi_i(\mathbf{m}_j)\cdot\mathbf{n}_j &= \delta_{ij}, \end{aligned} \tag{4.10}$$

where $\mathbf{m}_j$ denotes the midpoint of the j-th edge of the triangle and $\mathbf{n}_j$ the corresponding unit normal vector. This results in 21 shape functions which are illustrated in Figure 4.5 and Figure 4.6. For the explicit representation of the shape functions on the reference element see Appendix B. Due to high continuity requirements of these shape functions, it is rather difficult to transform them from the reference to the real triangle. However, there are computation techniques to realise this transformation for unstructured meshes. In this work, the Argyris element is implemented according to [17].

Then, a trial space V_h is used to construct an approximated function $v_h(x,t)$ via its basis

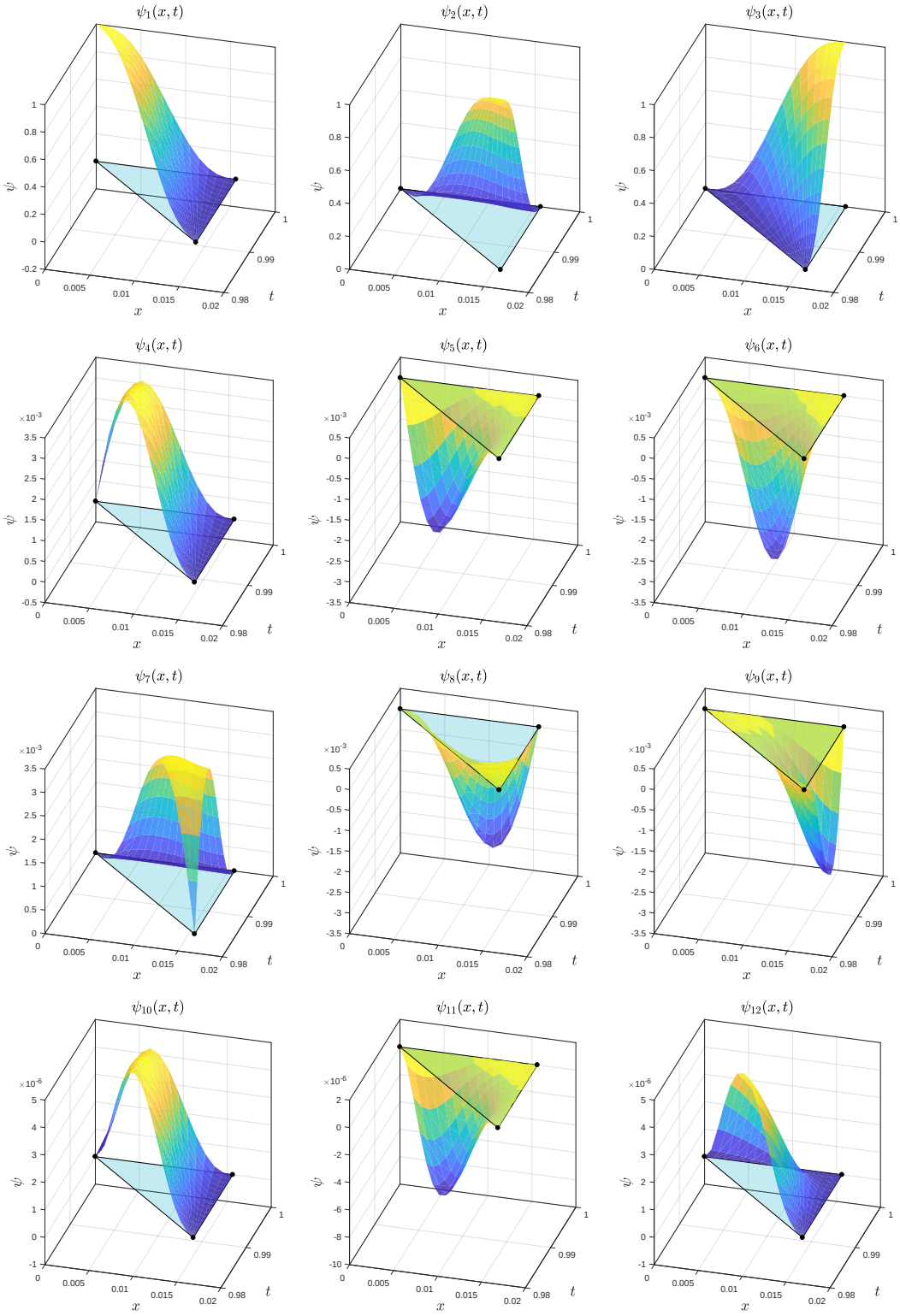

Figure 4.5: Argyris shape functions $\psi_j(x,t) \in \mathbb{P}^5(\tau_l)$ for $j \in \{1,...,12\}$

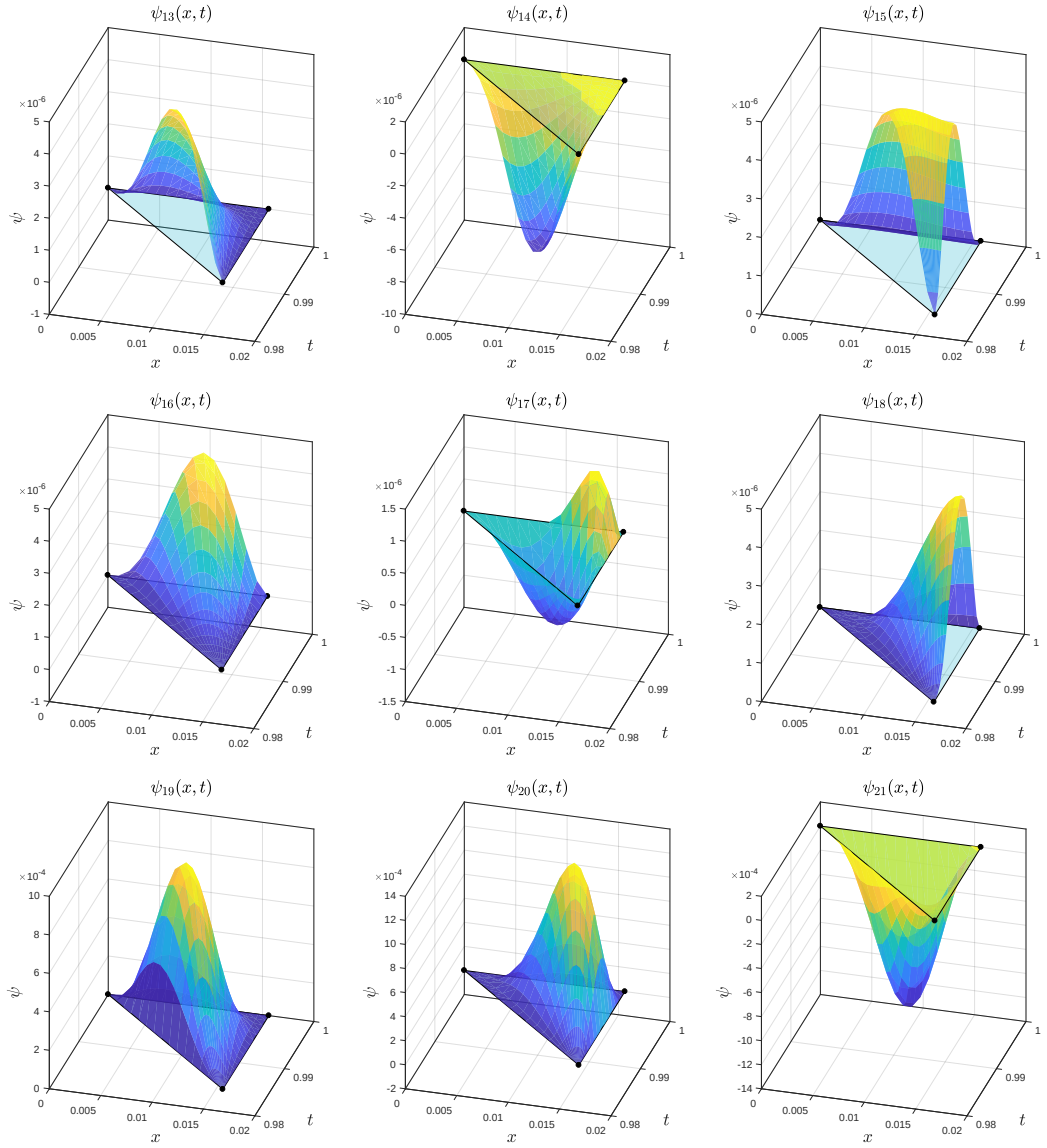

Figure 4.6: Argyris shape functions $\psi_j(x,t) \in \mathbb{P}^5(\tau_l)$ for $j \in \{13,...,21\}$

function. In particular, $v_h(x,t)$ is defined by

$$v_h(x,t) = \sum_{i=1}^{M} \varphi_i(x,t) v_i, \tag{4.11}$$

where v_i are constant scalar values and build the solution of the discrete variational problem. For more comprehensive information about finite elements see [11, 26].

To conclude this section we provide the definitions of all employed finite element spaces.

The space of discontinuous Lagrange polynomials of degree k on Q is given with

$$\mathcal{S}_h^{k,-1}(\mathcal{T}_N) = \{v \in L_2(\mathcal{T}_N) : v|_{\tau_l} \in \mathbb{P}^k(\tau_l),\ l = 1,...,N\}. \tag{4.12}$$

The space of continuous Lagrange polynomials on Q reads

$$\mathcal{S}_h^{k,0}(\mathcal{T}_N) = \{v \in C^0(\mathcal{T}_N) : v|_{\tau_l} \in \mathbb{P}^k(\tau_l),\ l = 1,...,N\} \subset H^1(Q). \tag{4.13}$$

The space of the Argyris elements on Q is given with

$$\mathcal{S}_h^{5,1}(\mathcal{T}_N) = \{v \in C^1(\mathcal{T}_N) : v|_{\tau_l} \in \mathbb{P}^5(\tau_l),\ l = 1,...,N\} \subset H^2(Q). \tag{4.14}$$

4.3 CG Method for the Elastic Bar

The derived Galerkin method for the elastic bar is transferred to discrete setting. Therefore, the trial space U is approximated with the finite element space from (4.14) and reads

$$U_h = \mathcal{S}_h^{5,1}(\mathcal{T}_N). \tag{4.15}$$

Consequently, the variational formulation (3.8) can be written in a discrete way: Find $u_h \in U_h$ such that

$$b(u_h, v_h) = \ell(v_h) \tag{4.16}$$

holds for all $v_h \in U_h$. We remark that the penalty parameter γ_B in (4.16) must be sufficiently small. In this work, γ_B is scaled according to the mesh size to obtain optimal convergence rates. In particular, we set $1/\gamma_B = 10^4 N^2$.

4.4 DPG Method for the Acoustic Fluid

We replace the trial space U with the finite element space $U_h \subset U$. Since, it is difficult to construct R directly we compute R_h by $R_h = \mathrm{D}_h(V_h)$ where $V_h \subset V$. Then, the variational problem in the ideal DPG method reads: Find $(u_h, v_h) \in U_h \times V_h$ such that

$$b((u_h, \mathrm{D}_h v_h), w_h) = \ell(w_h) \quad \forall w_h \in \mathrm{T}(U_h \times R_h). \tag{4.17}$$

As mentioned, the operator T is not known. Therefore, we approximate it with $\mathrm{T}_h : U_h \times R_h \to Y_h$ where $Y_h \subset W_h$ is an enriched finite element space. This leads to

$$(\mathrm{T}_h(u_h, r_h), w_h) = b((u_h, r_h), w_h) \quad \forall w_h \in Y_h. \tag{4.18}$$

Thus, the variational problem of the practical DPG method reads: Find $(u_h, v_h) \in U_h \times V_h$ such that

$$b((u_h, \mathrm{D}_h v_h), w_h) = \ell(w_h) \quad \forall w_h \in \mathrm{T}_h(U_h \times R_h). \tag{4.19}$$

The choice of the polynomial degree k for the trial spaces and test spaces is not straightforward. In [20], some remarks on this choice are given and a suggestion to obtain optimal convergence rates is made. Within this work we stay with their recommendation and use the following finite element spaces

$$\begin{aligned} U_h &= \mathcal{S}_h^{k,-1}(\mathcal{T}_N) \times \mathcal{S}_h^{k,-1}(\mathcal{T}_N), \\ V_h &= \mathcal{S}_h^{k+1,0}(\mathcal{T}_N) \times \mathcal{S}_h^{k+1,0}(\mathcal{T}_N), \\ Y_h &= \mathcal{S}_h^{k+2,-1}(\mathcal{T}_N) \times \mathcal{S}_h^{k+2,-1}(\mathcal{T}_N). \end{aligned} \tag{4.20}$$

When implementing $\mathrm{D}_h v_h$ one can observe that $\ker \mathrm{D}_h$ is non trivial. In order to take care of this null space we clear the space V_h of all basis functions which are zero on the element boundaries, since they are definitely in $\ker \mathrm{D}_h$. In particular, we replace V_h by $\widetilde{V}_h = V_h \setminus \{\varphi \in V_h : \varphi|_{\partial\tau} = 0 \quad \forall \tau \in \mathcal{T}_N\}$. However, this only takes care of the null space partly. We recall a simplified version of (3.19) given by

$$\int_{\partial\tau} (\rho_0 n_t - n_x) + (-n_x + \frac{1}{K} n_t) \, \mathrm{d}\partial\tau. \tag{4.21}$$

It can be observed instantly that for certain (n_x, n_t) and combinations of ρ_0 and K a non trivial kernel is obtained. Despite this behaviour, there are solving techniques to avoid this problem (*cf.* [20]). Since only the component U_h is of interest one can resort to the conjugated gradient method to obtain a solution despite the null space and extract the unique solution u_h afterwards. However, in this work we regularise the equation system by applying a penalty term on certain parts of the equation system. In particular, we add the mass matrix of the space $\widetilde{V}_h$ multiplied by a penalty parameter γ_P onto the part of the equation system associated to $b((0, \mathrm{D}_h v_h), w_h)$ for $w_h \in \mathrm{T}(\{0\} \times R_h)$. The penalty parameter γ_P must be sufficiently small, in all numerical examples we used $\gamma_P = 10^{-9}$.

4.4.1 Error Estimator

In order to obtain an error estimate for $u - u_h$ in U we recall the ideal DPG method

$$u_h \in U_h : \quad b((u_h, r_h), w_h) = \ell(w_h) \quad \forall w_h \in \mathrm{T}(U_h \times R_h). \tag{4.22}$$

By inserting $(u-u_h, r-r_h)$ in the trial to test operator it follows

$$b((u-u_h, r-r_h), w) = (\mathrm{T}(u-u_h, r-r_h), w)_W \quad \forall w \in W. \tag{4.23}$$

From (3.21) we can replace $b((u,r),w)$ by $\ell(w)$ and obtain

$$(\mathrm{T}(u-u_h, r-r_h), w)_W = \ell(w) - b((u_h, r_h), w) \quad \forall w \in W. \tag{4.24}$$

Thus, the exact solution u does not have to be known in order to calculate the estimate $\|\mathrm{T}(u-u_h, r-r_h)\|_W$. It is sufficient to compute u_h. Moreover, this error estimate has good properties which are shown in the following. From the boundedness and the inf-sup condition follows

$$c_E \|(u-u_h, r-r_h)\|_{U\times R} \leq \|\mathrm{T}(u-u_h, r-r_h)\|_W \leq c_S \|(u-u_h, r-r_h)\|_{U\times R}. \tag{4.25}$$

Consequently, the error in U can be estimated by $\mathrm{T}(u-u_h, r-r_h)$. Since, the test space is broken

$$\|\mathrm{T}(u-u_h, r-r_h)\|_W^2 = \sum_{\tau \in Q_h} \Big((\mathrm{T}(u-u_h, r-r_h))|_\tau, (\mathrm{T}(u-u_h, r-r_h))|_\tau \Big)_W \tag{4.26}$$

holds and we can formulate the element error by

$$\eta_\tau^2 = \|(\mathrm{T}(u-u_h, r-r_h))|_\tau\|_W^2. \tag{4.27}$$

Therefore, η_τ can be used as an *a posteriori* error estimate per element and used in algorithms for adaptive mesh refinements. In this work element subdivisions are done by the means of the newest vertex bisection (NVB) which is implemented according to [25].

5 VERIFICATION AND NUMERICAL EXAMPLES

In the course of this chapter, the previously introduced space-time finite element methods are applied to several examples. Therefore, a framework was implemented in MATLAB. Within this framework classes for meshes, finite element spaces, etc. were written to obtain an object oriented application for finite element computations. Additionally, methods for plotting, assembling, evaluating form functions and so forth were implemented. We remark that for evaluating integrals standard Gauß-Legendre quadrature rules are used.

5.1 Wave Equation for the Elastic Bar

This section covers the numerical examples for the mechanical problem setting of the elastic bar where the derived CG method is verified and two different numerical experiments are investigated. In particular, an initial boundary value problem is considered in subsections 5.1.2 and 5.1.3 where a wave front enters the space-time domain.

5.1.1 Verification

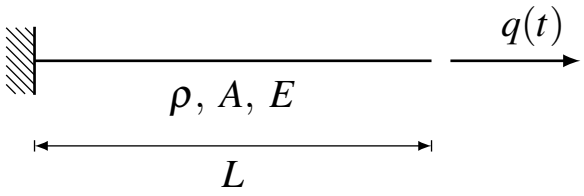

Figure 5.1: Elastic bar

We consider a mixed problem meaning we impose a Dirichlet and Neumann type boundary condition with the given setting as depicted in Figure 5.1. No damping is imposed and ρ, E, A, L, T are set to unit values which leads to the governing equation

$$\partial_{tt} u - \partial_{xx} u = 0. \tag{5.1}$$

We obtain a solution via the representation formula (*cf.* [2]) given with

$$u(x,t) = \int_0^{t+x-1} q(\lambda)\,\mathrm{d}\lambda, \tag{5.2}$$

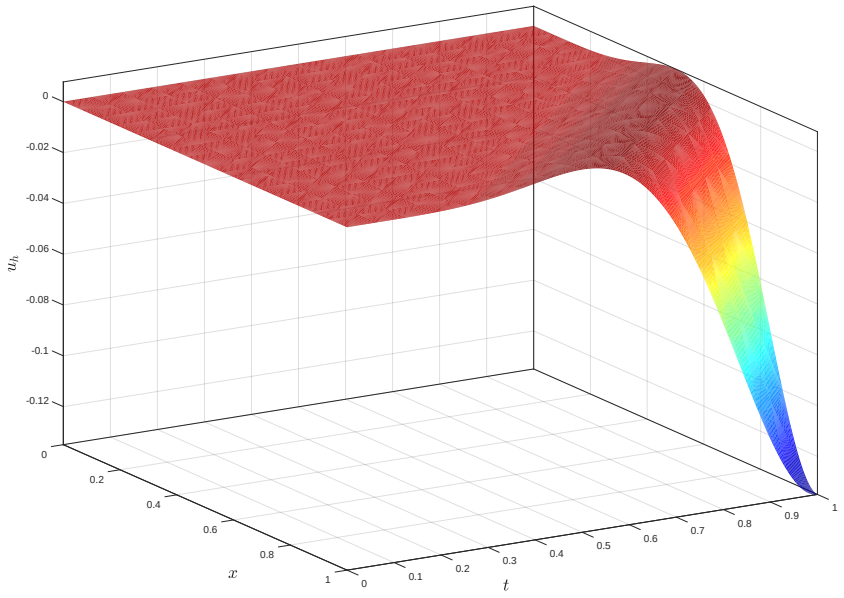

Figure 5.2: Approximated displacement $u_h(x,t)$ for a smooth exact solution $u(x,t)$

for $x \in \Omega = (0,L)$ and $t \in \Upsilon = (0,T)$. The initial conditions are given with $u_0(x) = 0$ and $\dot{u}(x) = 0$ for $x \in \Omega$ while the Dirichlet condition is $\tilde{u} = 0$ for $t \in \Upsilon$. The loading on the Neumann type boundary is set to

$$q(t) = t^3 \sin(2\pi t), \tag{5.3}$$

where $t \in \Upsilon$. This example serves the purpose of verification. We use a standard triangulation for the space-time domain $Q = \Omega \times \Upsilon$ and conduct a convergence study using uniform mesh refinements. Exemplary, an approximate solution $u_h(x,t)$ for $N = 2048$ elements is depicted in Figure 5.2. We verify the implementation by investigating the experimental rate of convergence (*eoc*) of the error in the $L_2(Q)$ norm given by $\|u - u_h\|_{L_2(Q)}$. In Table 5.1 the L_2-error and the *eoc* in mesh size h are displayed for uniform mesh refinements. As expected the full rate of convergence $k+1 = 6$ for $\|u - u_h\|_{L_2(Q)}$ is obtained. This is due to the sufficiently smooth solution which allows for the optimal convergence rates of the finite element space $\mathcal{S}_h^{5,1}(Q)$ of the Argyris element which is of polynomial degree $k = 5$. Moreover, it can be observed in Table 5.1 that good technical solutions can be obtained already with 32 elements. Here, the relative error amounts to 0.11% only.

N	M	$\|u-u_h\|_{L_2(Q)}$	eoc
2	29	3.792e-03	-
8	70	6.677e-05	5.828
32	206	2.332e-06	4.839
128	694	2.310e-08	6.658
512	2534	2.961e-10	6.285
2048	9670	4.114e-12	6.169
8192	37766	6.044e-14	6.089

Table 5.1: Convergence study on uniform meshes

5.1.2 Wave Front with Damping

In the second example we deploy a similar setting, the material parameters ρ, E, A, L are set to unit values while the end time is given with $T = 1$. The propagation velocity of the wave is given with $c = \sqrt{\frac{E}{\rho}} = 1$. However, a small value for the viscosity is defined with $D = 10^{-3}$. Given this setting we construct a Dirichlet boundary value problem with zero

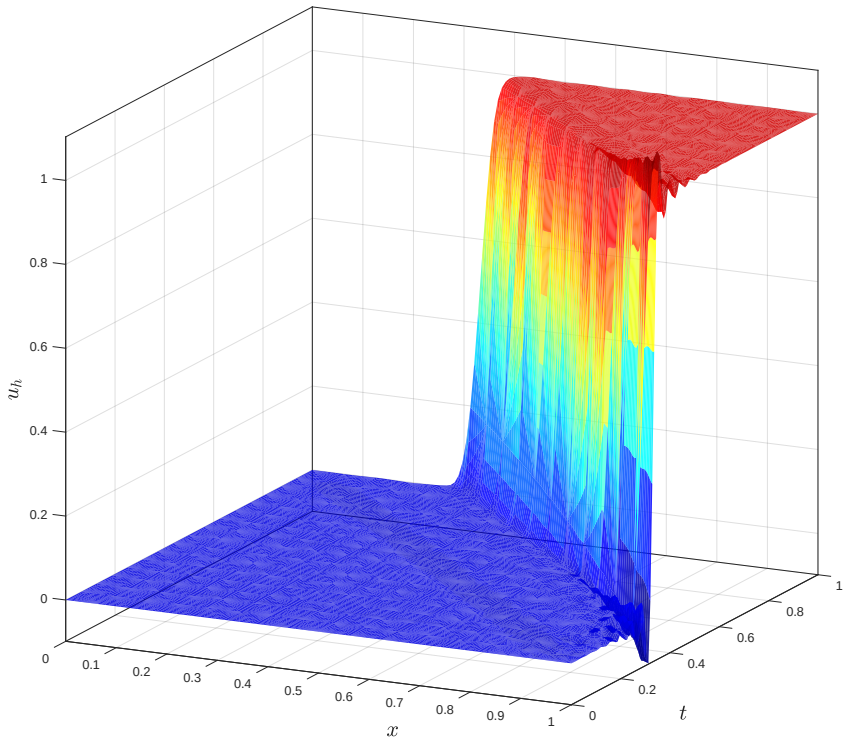

Figure 5.3: Approximated solution $u_h(x,t)$ for a wave propagation with damping

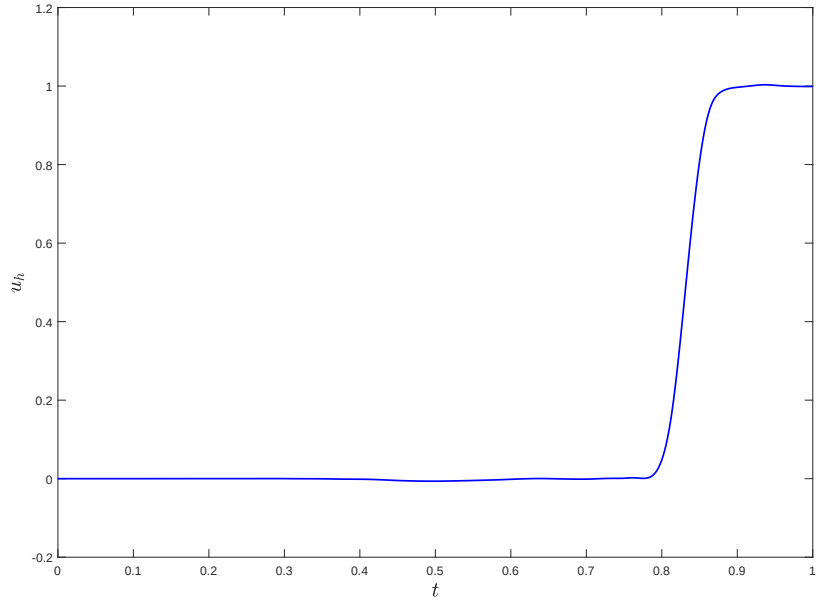

Figure 5.4: Approximated solution $u_h(\frac{L}{2},t)$

initial conditions. On the lateral boundary Σ of the space time domain Q the boundary displacement $\tilde{u}(t)$ is defined by

$$\begin{aligned} \tilde{u}_0(t) &= 0, \\ \tilde{u}_L(t) &= H(t-\frac{1}{3}), \end{aligned} \tag{5.4}$$

for $t \in (0,1)$ and where $\tilde{u}_0$ denotes the Dirichlet data at $x = 0$ and $\tilde{u}_L$ the Dirichlet data at $x = L$. Note that $H(t)$ denotes the Heaviside step function. On the initial boundary Ω_0 of the space time domain Q we impose

$$\begin{aligned} u_0(x) &= 0, \\ \dot{u}_0(x) &= 0, \end{aligned} \tag{5.5}$$

for $x \in (0,1)$. An approximated solution $u_h(x,t)$ is obtained as depicted in Figure 5.3. It can be observed that the solution at $x = L$ of the space time domain oscillates, although here the solution is given by the boundary condition $\tilde{u}_L(t)$. These oscillations occur because the given trial space cannot resolve the space of solution and because stability problems arise due to the imposing of the boundary conditions via the penalty method. However, the given viscosity smooths the displacement field which can be observed in Figure 5.4 as the wave propagates through the space time domain resulting in a good technical approximation.

5.1.3 Wave Front without Damping

The restrictions of the derived CG method are showcased in this example. We consider the same setting as in the last example $Q = (0,1)^2$ with the exception of the viscosity which is set to zero $D = 0$. Here, an exact solution is given by

$$u(x,t) = H((x - \frac{4}{3}) + t), \tag{5.6}$$

where $x = \frac{4}{3}$ represents a source position. The exact solution from (5.6) leads to the same initial and boundary conditions as observed in (5.4) and (5.5). As seen in Figure 5.5 the approximated displacement field $u_h(x,t)$ oscillates strongly around the exact solution $u(x,t)$ which is depicted in Figure 5.6. This results in discrepancies between the approximated solution $u_h(x,t)$ and the exact solution $u(x,t)$ most notably around the discontinuity. This is due to the fact that the space of the Argyris elements is not able to resolve such a rough solution. Additionally, it can be seen that the approximated solution differs from the exact solution at the lateral boundary of the space-time domain although $u_h(x,t)$ is given

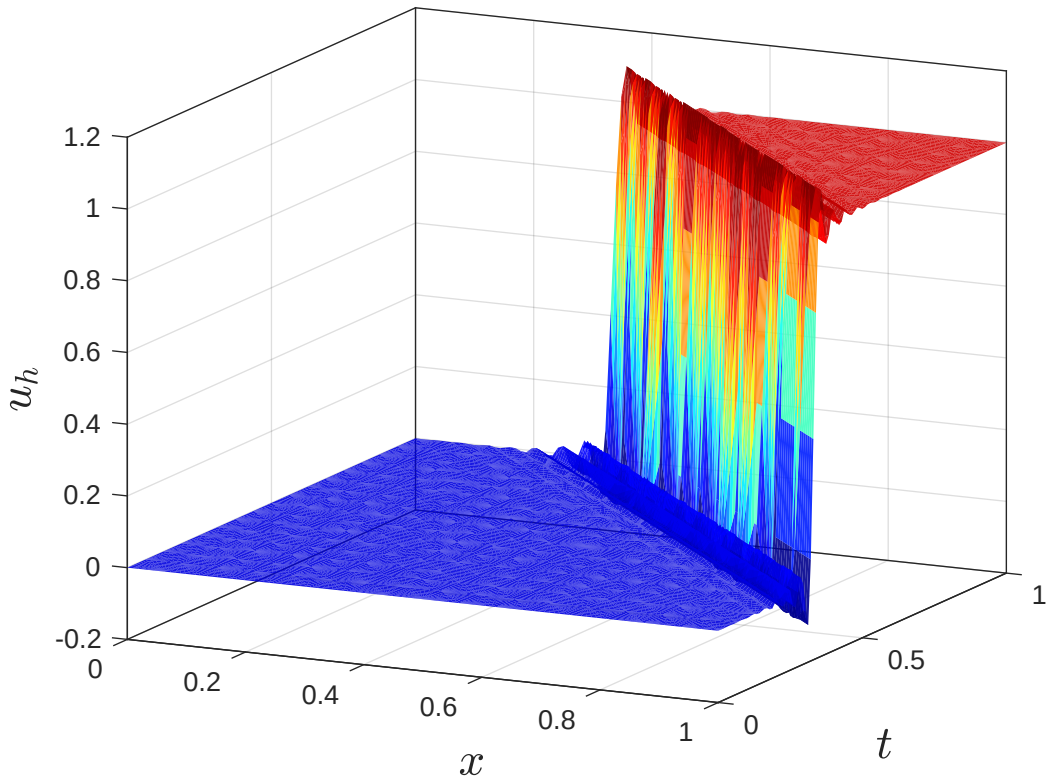

Figure 5.5: Approximated solution $u_h(x,t)$ for a wave propagation without damping

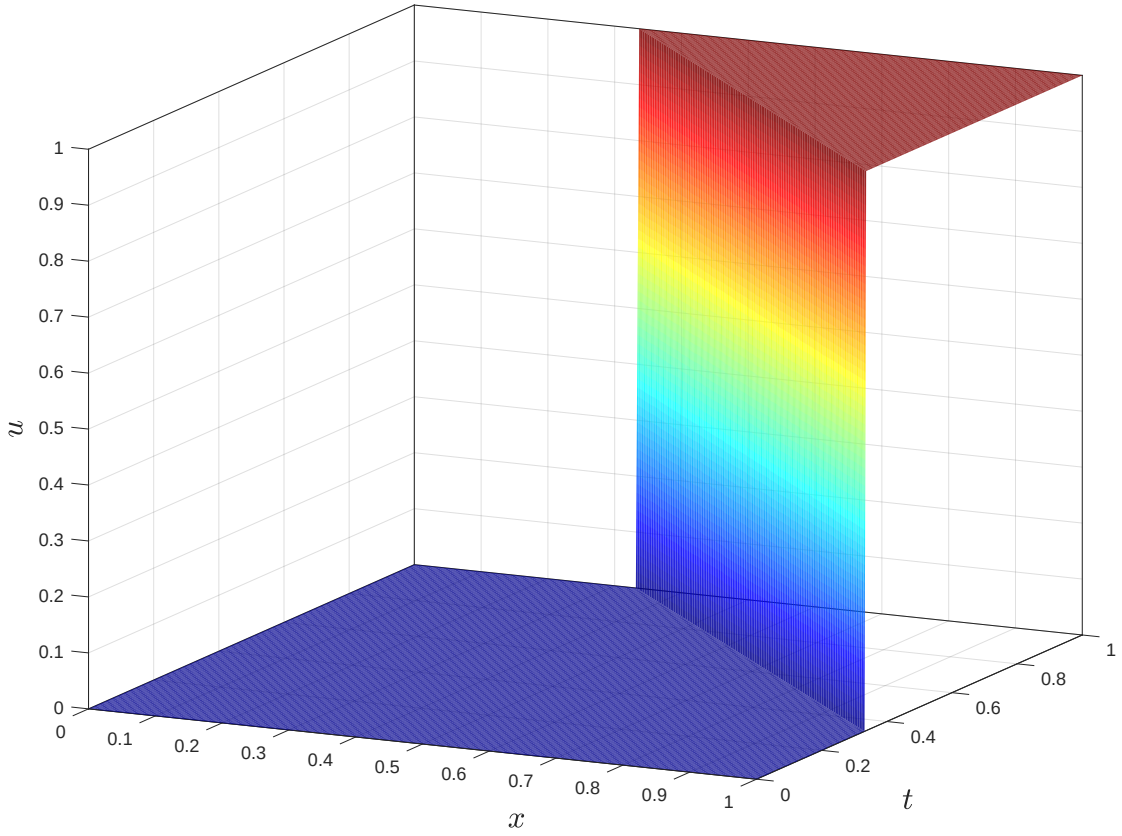

Figure 5.6: Exact solution $u(x,t)$

by the boundary condition there. This behaviour arises since the boundary conditions are imposed via the penalty method.

5.2 Wave Equation for the Acoustic Fluid

In this section the DPG method for the acoustic fluid is investigated. We proceed in as in section 5.1 verifying the DPG method and analysing two numerical examples. As before subsections 5.2.2 and 5.2.3 cover a wave front which enters the space-time domain.

5.2.1 Verification

The first example for the acoustic fluid is used to verify the presented approach. We stick to the space-time domain $Q = (0,1)^2$ and set ρ_0 and K to unit values. Furthermore, we consider a problem with initial and boundary conditions equal to zero. The governing system of equations is given by

$$\begin{aligned} \partial_t v - \partial_x p &= f \quad \text{in } Q, \\ \partial_t p - \partial_x v &= g \quad \text{in } Q. \end{aligned} \tag{5.7}$$

We use the method of manufactured solutions and obtain an analytical solution for $v(x,t)$ and $p(x,t)$ given by

$$\begin{bmatrix} v \\ p \end{bmatrix} = \begin{bmatrix} \sin(\pi x)\sin^2(\pi t) \\ \sin(\pi x)\sin^2(\pi t) \end{bmatrix}, \tag{5.8}$$

for $(x,t) \in Q$. Once observe in (5.8) that this solution fulfils the initial and boundary conditions. Using (5.8) in (5.7) gives the following loading functions

$$\begin{aligned} f(x,t) &= \pi \sin(\pi t)\Big[2\sin(\pi x)\cos(\pi t) - \cos(\pi x)\sin(\pi t)\Big], \\ g(x,t) &= \pi \sin(\pi t)\Big[2\sin(\pi x)\cos(\pi t) - \cos(\pi x)\sin(\pi t)\Big]. \end{aligned} \tag{5.9}$$

After discretizing the space-time domain a convergence study is conducted. We use an uniform mesh refinement and increase the polynomial degree k of the trial space. Exemplary, an approximated solution for $p_h(x,t)$ of the polynomial degree $k = 0$ for the trial space is depicted in Figure 5.7a and for $k = 1$ in Figure 5.7b. Note that a standard triangulation

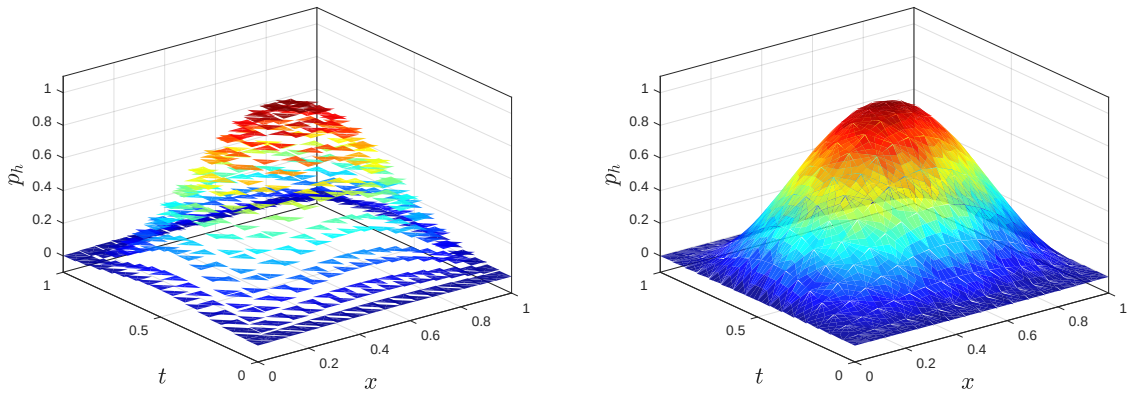

(a) Piecewise constant (b) Piecewise linear

Figure 5.7: Approximated solution for the pressure $p_h(x,t)$

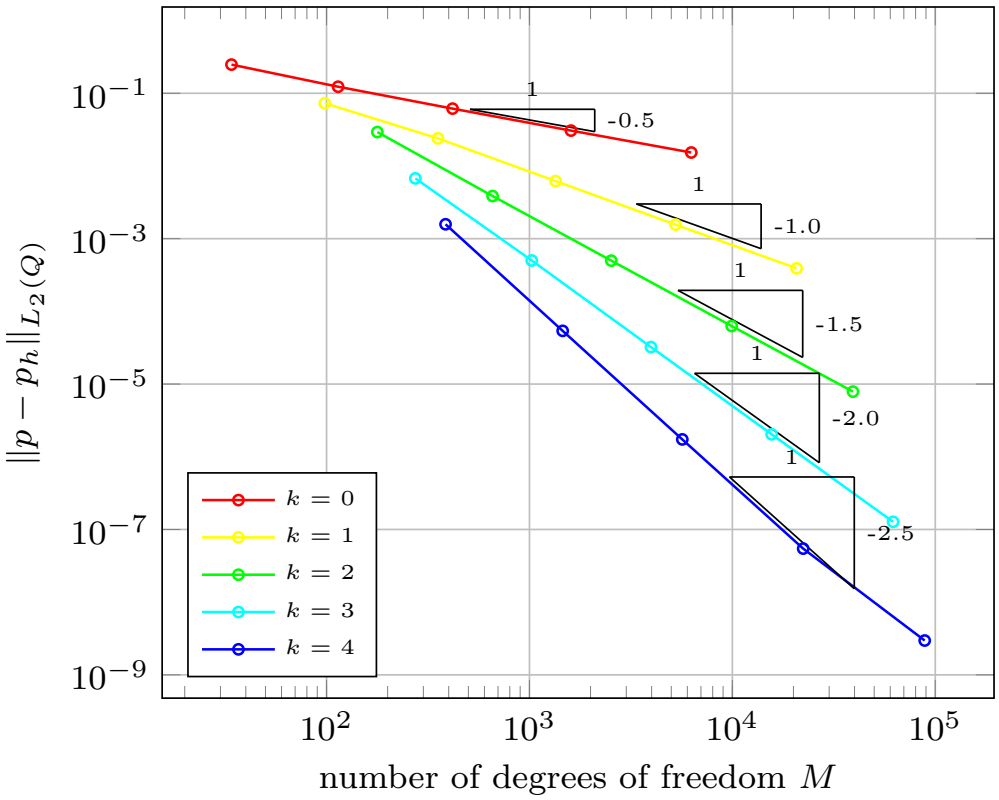

Figure 5.8: *eoc* for different polynomial degrees

with $N = 512$ elements for both approximations is deployed. Furthermore, in Figure 5.8 the error in the L_2-norm $\|p - p_h\|_{L_2(Q)}$ for the trial space where $k \in \{0,1,2,3,4\}$ is displayed. One can observe the increase of the *eoc* according to the polynomial degree k of the trials space. We remark that the *eoc* which is used here relates to the number of degrees of freedom (eoc_M) and not to the mesh size (eoc_h). However, eoc_M is proportional to eoc_h. This relation is given by

$$eoc_h \sim 2eoc_M. \tag{5.10}$$

From here on *eoc* refers to eoc_M.

5.2.2 Wave Front

In this numerical example we construct the same setting as presented in 5.1.3, where a wave front enters the space-time domain $Q = (0,1)^2$. This leads with the given material

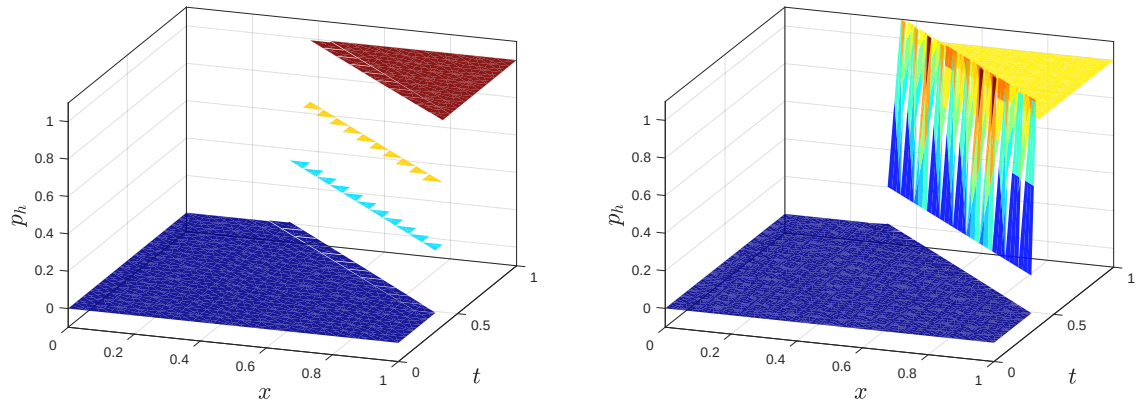

(a) Piecewise constant (b) Piecewise linear

Figure 5.9: Approximated solution for the pressure $p_h(x,t)$

parameters to the governing system of equations

$$\begin{aligned} \partial_t v - \partial_x p &= 0 \quad \text{in } Q, \\ \partial_t p - \partial_x v &= 0 \quad \text{in } Q. \end{aligned} \tag{5.11}$$

For this problem setting the exact solutions $p(x,t)$ and $v(x,t)$ are given by

$$p(x,t) = v(x,t) = H((x - \frac{4}{3}) + t), \tag{5.12}$$

for $(x,t) \in Q$. We remark that (5.12) and (5.6) coincide. The boundary and initial conditions are given directly from the analytical solutions $p(x,t)$ and $v(x,t)$. We conduct a convergence study by increasing the polynomial degree of the trial space and by refining the mesh uniformly. In Figures 5.9a and 5.9b an approximate solution on a mesh with $N = 512$ elements using trial spaces with $k = 0$ and $k = 1$ is depicted. Since the DPG method is formulated in a broken space the discontinuity produced by the wave is resolved nicely and in contrast to the CG method in example 5.1.3. However, using an uniform refinement here leads not to full convergence rates. In case of $k = 0$ only an $eoc = 0.25$ is achieved.

5.2.3 Adaptivity

The last example illustrates the potential of local refinement for solutions with local features such as the analytical solution (5.6) of the investigated initial boundary value problem from subsection 5.1.3 and 5.2.2. Again, we assume the same problem setting as in subsection 5.2.2 with $Q = (0,1)^2$ and the analytical solution (5.12). An adaptive method is

conducted where the error estimate from subsection 4.4.1 is used. Furthermore, in this example $k = 0$ is used. The initial configuration of setting is depicted in Figure 5.10a. We compute the DPG error indicator η from (4.27) for each element. Then, all elements hav-

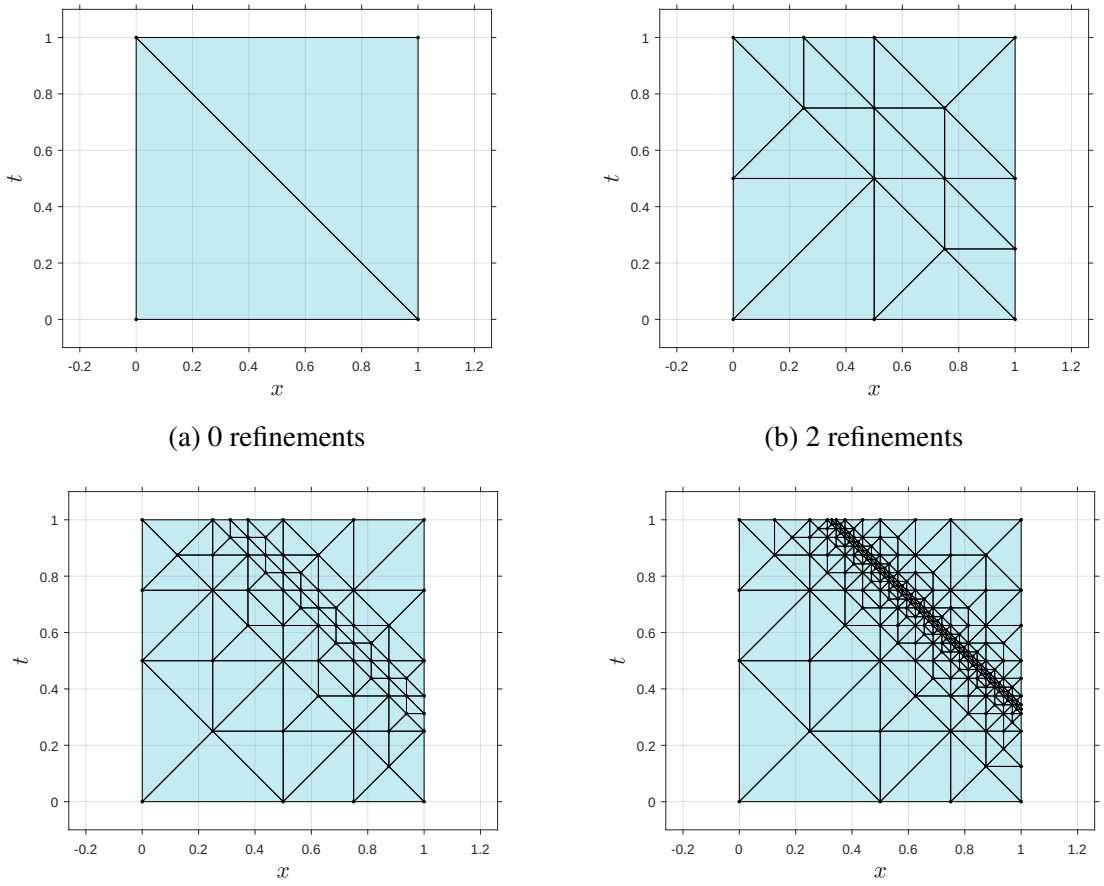

(a) 0 refinements

(b) 2 refinements

(c) 4 refinements

(d) 6 refinements

Figure 5.10: Adaptive refinement with polynomial degree of $k = 0$

ing an error which is greater than 50% of the total indicated error are marked and refined. As Figures 5.10a to 5.10d show, the wave front is resolved by local refinements. Although this is an artificial example where the error appears only in elements at the jump of the Heaviside one can observe an increase in the *eoc* using an adaptive scheme. A comparison of the $L_2(Q)$-error between an uniform and adaptive refinement can be seen in Figure 5.11. Thus, good technical approximations without refining the whole space-time domain can be obtained if only certain sub domains show specific behaviour.

Lastly, we show the potential of adaptivity for an example which cannot be represented

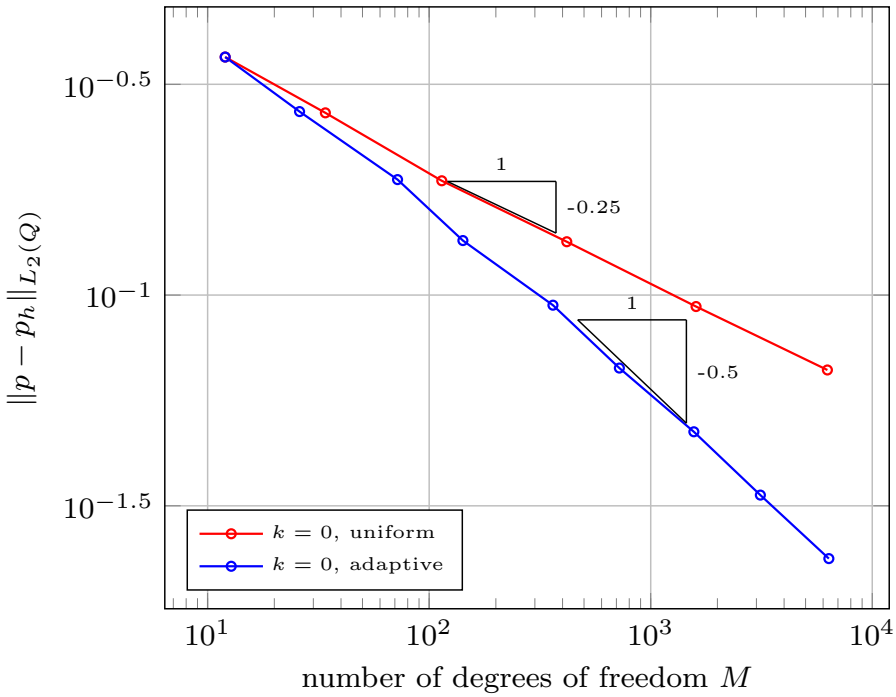

Figure 5.11: Comparison between uniform and adaptive refinement

exactly by piecewise polynomials. We stay in the setting $Q = (0,1)^2$ with the same material parameters and $f(x,t) = g(x,t) = 0$. We construct a solution with the function

$$\lambda(\xi) = H(\xi)|\sin(\frac{3}{2}\pi\xi)|. \tag{5.13}$$

Then, an exact solution for this problem setting can be given with

$$p(x,t) = v(x,t) = \lambda(x - \frac{2}{3} + t), \tag{5.14}$$

for $(x,t) \in Q$. This solution has kinks because of the absolute value function and cannot be represented exactly by piecewise polynomials because of the sine function. Therefore, we make use of a higher polynomial degree and approximate this solution with $k = 2$. We deploy an adaptive refinement starting with the same initial configuration as in last example. Here, all elements having an error above 60% of the total indicated error are refined. In Figures 5.12a - 5.12d the mesh of each refinement step is depicted. The discontinuity of the solution is resolved well by the local refinements. In Figure 5.13 the approximated solution $u_h(x,t)$ after 8 refinement steps is shown. One can observe the two kinks of the solution travelling through the space-time domain and smoothness of the solution in between. The potential of the DPG method can be seen in this example since the mesh can be refined adaptively for rough local features and a high polynomial degree for smooth features of the solution can be utilised.

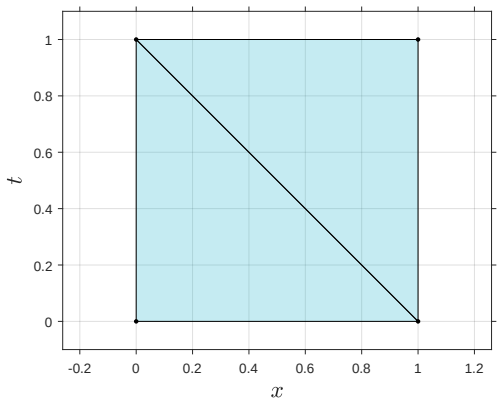

(a) 0 refinements

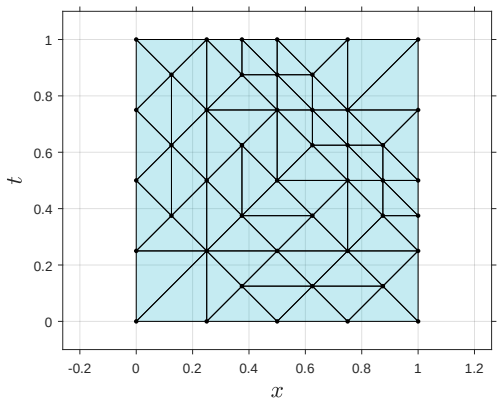

(b) 4 refinements

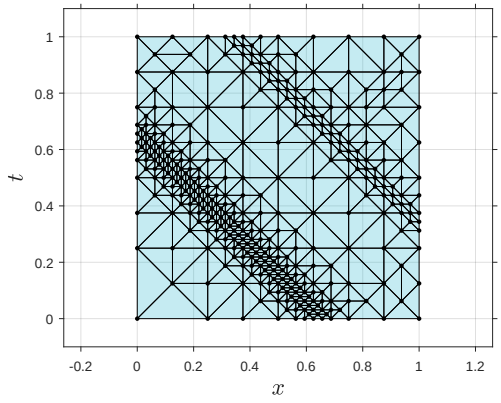

(c) 8 refinements

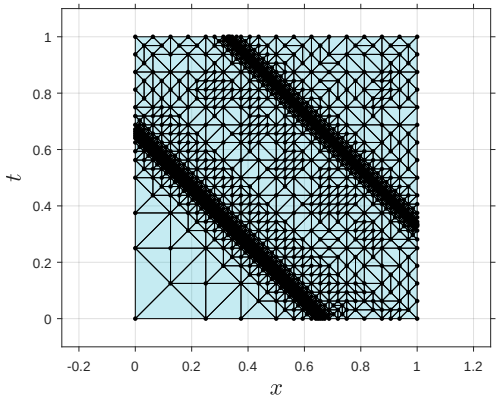

(d) 12 refinements

Figure 5.12: Adaptive refinement with polynomial degree of $k = 2$

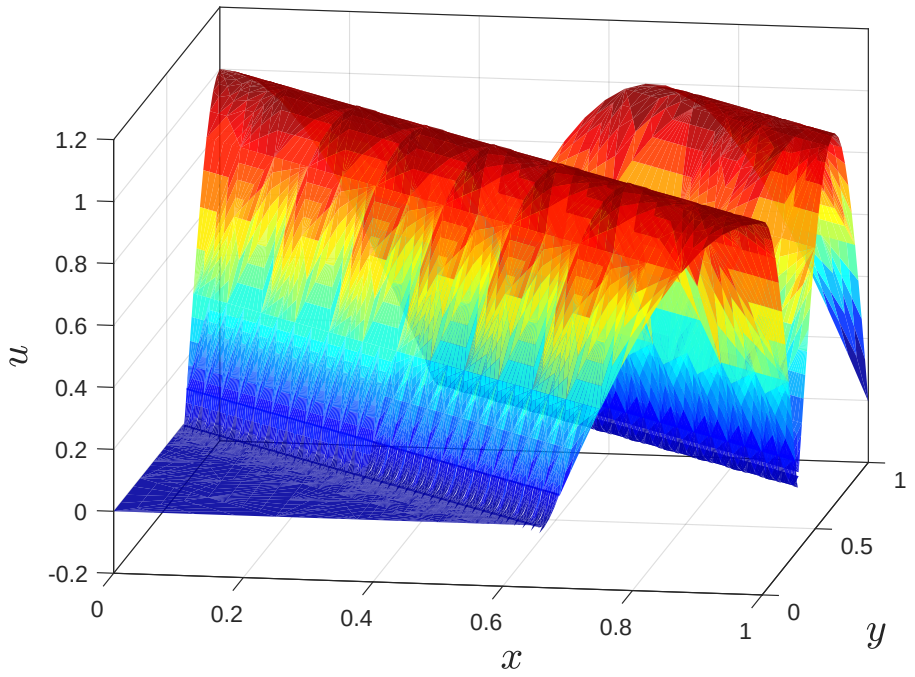

Figure 5.13: Approximated solution $p_h(x,t)$ after 8-the refinement step

6 CONCLUSION

In the course of this work two different space-time formulations for time dependent mechanical problems have been presented and investigated. In Chapter 2, the wave equation for the elastic bar and the first order system of the wave equation for the acoustic fluid have been derived. Assuming linear kinematic behaviour as well as linear elastic constitutive behaviour, all derived governing partial differential equations are linear. A variational formulation for both mechanical problems was introduced in Chapter 3 leading to a Bubnov Galerkin method for the elastic bar and a discontinuous Petrov Galerkin method for the acoustic fluid. The most notable difference between classic approaches and the ones presented here is the discretization technique. Space-time methods discretize $\Omega \times \Upsilon$ as a whole. In contrast to classic methods which discretize the spatial domain Ω and the time domain Υ separately. Here, an approximation over the spatial domain at every time can be calculated. This allows for unstructured triangulations over the space-time domain Q and more importantly the possibility for local refinement in space-time. Discretization techniques and a short introduction on finite elements were given in Chapter 4. Both methods have been studied and verified. Several numerical examples were shown and investigated in Chapter 5. As expected all obtained convergence rates matched their respective theoretical rate.

We summarise shortly the advantages and disadvantages of both methods. With the continuous Galerkin method for the elastic bar it was possible to obtain numerical solutions with high convergence orders given a sufficiently smooth enough analytical solution. However, problems arise when approximating rough solutions due to the high continuity requirements of the trial space. Furthermore, imposing initial and boundary conditions by the penalty method can lead to stability problems of the method. The discontinuous Petrov Galerkin method has the ability to resolve rough solutions due to the broken formulation. Moreover, the rate of convergence can be increased by increasing the polynomial degree of the trial space. One important feature of the method is also the potential for local mesh refinements since an efficient error estimate is directly given by the method. Therefore, it was without effort to conduct an adaptive scheme for physical problems with local features in the solution. One drawback of this method is that an equation system has to be solved to obtain the test functions. However, this computational effort is insignificant since this equation system can be solved locally and, thereby, in parallel.

A MATHEMATICAL PRELIMINARIES

An overview of mathematical definitions is given here which are partly adapted from [21, 37].

In this line of work only the field of real numbers $\mathbb{R}$ is considered.

Definition A.1 (Vector space) *Let V be a set with real numbers $\mathbb{R}$ as its field, a vector addition $+ : V \times V \to V$ and a scalar multiplication $\cdot : \mathbb{R} \times V \to V$. Then $(V, +, \cdot)$ is called a vector space over $\mathbb{R}$ if the vector addition satisfies*

$$\begin{aligned} u + (v + w) &= (u + v) + w, && \textit{associativity} \\ u + v &= v + u, && \textit{commutativity} \\ v + 0 = 0 + v &= v, && \textit{existence of neutral element } 0 \in V \\ v + (-v) = (-v) + v &= 0, && \textit{existence of inverse element } -v \in V \end{aligned}$$

for all $u, v, w \in V$, and the scalar multiplication satisfies

$$\begin{aligned} \lambda \cdot (u + v) &= \lambda \cdot u + \lambda \cdot v, && \textit{left distributive property} \\ (\lambda + \mu) \cdot v &= \lambda \cdot v + \mu \cdot v, && \textit{right distributive property} \\ (\lambda \mu) \cdot v &= \lambda \cdot (\mu \cdot v), && \textit{compatibility} \\ 1 \cdot v &= v, && \textit{neutrality of } 1 \in \mathbb{R} \end{aligned}$$

for all $u, v \in V$ and $\lambda, \mu \in \mathbb{R}$.

Definition A.2 (Scalar product) *A mapping $(\cdot, \cdot) : V \times V \to \mathbb{R}$ is called scalar product if*

$$\begin{aligned} (v, v) \geq 0 \quad \wedge \quad (v, v) = 0 \quad \Leftrightarrow \quad v = 0, && \textit{positive definiteness} \\ (u, v) = (v, u), && \textit{symmetry} \\ (\lambda u, v) = \lambda (u, v), && \textit{linearity in the first argument} \\ (u + v, w) = (u, w) + (v, w), && \textit{linearity in the first argument} \end{aligned}$$

for all $u, v, w \in V$ and $\lambda \in \mathbb{R}$.

From symmetry and linearity in the first arguments follows linearity in the second argument. A vector space with a scalar product is called pre-Hilbert space.

Definition A.3 (Norm) *A mapping* $\|\cdot\| : V \to \mathbb{R}_{\geq 0} := \{x \in \mathbb{R} : x \geq 0\}$ *is called norm if*

$$\begin{aligned} \|v\| = 0 \quad &\Leftrightarrow \quad u = 0, && \textit{definiteness} \\ \|\lambda \cdot v\| &= |\lambda| \|v\|, && \textit{absolute homogeneity} \\ \|u+v\| &\leq \|u\| + \|v\|, && \textit{triangle inequality} \end{aligned}$$

holds for all $u, v \in V$ *and* $\lambda \in \mathbb{R}$.

The scalar product induces a norm on a vector space $\|\cdot\| = \sqrt{(\cdot,\cdot)}$. A vector space with a norm is called normed space.

Remark A.1 *A pre-Hilbert space V with induced norm is a normed space and the Cauchy-Schwarz inequality holds*

$$|(u,v)| \leq \|u\| \|v\|$$

for all $u, v \in V$.

Definition A.4 (Hilbert space) *A Hilbert space is a complete pre-Hilbert space.*

For a rigorous definition the interested reader is referred to [21]. From here on we restrict the exposition to Hilbert spaces only.

Definition A.5 (Linear operator) *Let U and V be vector spaces. A mapping* $\mathrm{T} : U \to V$ *is called linear if*

$$\begin{aligned} \mathrm{T}(u+v) &= \mathrm{T}u + \mathrm{T}v, \\ \mathrm{T}(\lambda u) &= \lambda \cdot \mathrm{T}u, \end{aligned}$$

for $u, v \in \mathrm{dom}\,\mathrm{T}$ *and* $\lambda \in \mathbb{R}$.

In above definition $\mathrm{dom}\,\mathrm{T}$ denotes the domain of definition of T. Furthermore, the range of T is defined by

$$\mathrm{ran}\,\mathrm{T} = \{v \in V : \exists u \in \mathrm{dom}\,\mathrm{T} : \mathrm{T}u = v\},$$

and the null space or kernel of T is defined by

$$\ker \mathrm{T} = \{u \in \mathrm{dom}\,\mathrm{T} : \mathrm{T}u = 0\}.$$

Definition A.6 (Bounded operator) *Let U and V be Hilbert spaces. A mapping $\mathrm{T} : U \to V$ is called bounded if there exists a $c \geq 0$ such that*

$$\|\mathrm{T}u\|_V \leq c\|u\|_U$$

for all $u \in \mathrm{dom}\,\mathrm{T}$.

Further, let $\mathcal{L}(U,V) = \{\mathrm{T} : U \to V$, bounded linear and $\mathrm{dom}\,\mathrm{T} = U\}$ be the space of bounded linear operators from U to V defined on U. From here on we only consider operators $\mathrm{T} \in \mathcal{L}(U,V)$.

Definition A.7 (Linear form) *A linear form is a bounded linear operator that maps from a vector space to its field $\ell : V \to \mathbb{R}$.*

Definition A.8 (Bijection) *The mapping $\mathrm{T} : U \to V$ is bijective if it is surjective and injective. The mapping T is surjective if $\mathrm{ran}\,\mathrm{T} = V$ and injective if from $\mathrm{T}x = \mathrm{T}y$ follows $x = y$.*

Note that a linear operator T is injective if and only if $\ker \mathrm{T} = \{0\}$.

Definition A.9 (Isometric isomorphism) *A mapping $\mathrm{T} : U \to V$ is an isometric isomorphism if T is bijective and norm preserving which means*

$$\|\mathrm{T}u\|_V = \|u\|_U,$$

for all $u \in U$.

Definition A.10 (Dual space) *A dual space $V^* = \mathcal{L}(V,\mathbb{R})$ is the space of all linear forms on the vector space V.*

Theorem A.1 (Riesz representation theorem) *Let V be a Hilbert space. Then $\mathrm{R}_V : V \to V^*$ defined by*

$$v \mapsto \mathrm{R}_V v, \qquad (\mathrm{R}_V v)(u) = (u,v),$$

for all $u,v \in V$ is an isometric isomorphism. This means for every $u^* \in V^* = \mathcal{L}(V,\mathbb{R})$ exists one and only one $v \in V$ with $u^*(u) = (u,v)$ and $\|v\|_V = \|u^*\|_{V^*}$.

For the proof see [21].

Definition A.11 (Bilinear form) *A bilinear form maps two vector spaces to their common field $b : U \times V \to \mathbb{R}$, which is linear with respect to its first and second argument.*

Function spaces are vector spaces with functions as elements. In the following, we introduce some function spaces which are used later on.

Definition A.12 (C^p function space) *The space of p-times continuously differentiable scalar-valued functions $v : \Omega \subset \mathbb{R}^d \to \mathbb{R}$ is defined by*

$$C^p(\Omega) = \{v : v \text{ is } p\text{-times continuously differentiable}\}.$$

Definition A.13 (L_2 function space) *The space $L_2(\Omega)$ is the space of square integrable functions on a domain Ω. It is a Hilbert space and defined by*

$$L_2(\Omega) = \{v : \int_\Omega [v(x)]^2 \, \mathrm{d}x < \infty\}.$$

Definition A.14 (H^p function space) *The space $H^p(\Omega)$ is the space of square integrable functions on a domain Ω which has square integrable weak derivatives up to order p and is defined by*

$$H^p(\Omega) = \{v : D^\alpha v \text{ exists and } D^\alpha v \in L_2(\Omega) \; \forall \alpha : |\alpha| \leq p\},$$

The weak differential operator D^α is defined as in [34].

As mentioned in the introduction in this work, variational formulations are applied on mechanical problems. Therefore, a short overview on variational problems is given. Let U, V be Hilbert spaces and $b : U \times V \to \mathbb{R}$ a bilinear form. For given $\ell \in V^*$ the variational problem reads

$$\text{Find } u \in U : b(u,v) = \ell(v) \quad \forall v \in V,$$

The variational problem is well-posed (there exists a unique solution $u \in U$ for any $\ell \in V^*$) if and only if

- b is bounded, which means there exists a $c_S \geq 0$ such that

$$b(u,v) \leq c_S \|u\|_U \|v\|_V, \quad \forall u \in U, v \in V,$$

- the inf-sup conditions holds, which means there exists a $c_E > 0$ such that

$$\begin{aligned} \forall u \in U \quad \exists v \in V \ : \quad b(u,v) &\geq c_E \|u\|_U \|v\|_V \\ &\Leftrightarrow \\ \sup_{v \in V \setminus \{0\}} \frac{b(u,v)}{\|v\|_V} &\geq c_E \|u\|_U, \quad \forall u \in U \\ &\Leftrightarrow \\ \inf_{u \in U \setminus \{0\}} \sup_{v \in V \setminus \{0\}} \frac{b(u,v)}{\|u\|_U \|v\|_V} &\geq c_E, \end{aligned}$$

- for every $v \in V \setminus \{0\}$ there exists a $u \in U$ such that

$$b(u,v) \neq 0.$$

Furthermore, this leads to the stability relation

$$\|u\|_U \leq \frac{1}{c_E} \|\ell\|_{V^*}.$$

For further information of the well-posedness of variational formulations the reader is referred to [9, 10].

B EXPLICIT SHAPE FUNCTIONS

Here, we give some remarks on shape functions. In particular, an introduction of the Lagrangian shape functions and the Argyris shape functions in the reference element is given. For further information and a more comprehensive definition on Lagrangian shape functions see, e.g. [9,26]. Definitions of the Argyris element can be found in [4,17,26].

B.1 Lagrangian Shape Functions

First, we describe the definition of the shape functions in the linear case. In this case, there are three shape functions ψ_i, each described by three coefficients $c_{i,j}$. Then, the i-th shape function ψ_i is given with

$$\psi_i(\xi,\eta) = c_{1,i} + c_{2,i}\xi + c_{3,i}\eta,$$

for $(\xi,\eta) \in \hat{\tau}$. The coefficients $c_{i,j}$ are, then, obtained by solving the problem (4.8). This leads in the linear case to the matrix

$$\mathrm{C} = \begin{bmatrix} 1 & 0 & 0 \\ -1 & 1 & 0 \\ -1 & 0 & 1 \end{bmatrix}.$$

In order that this problem is well-posed. The number of Nodes must coincide with the number of shape functions. This implies that the coefficient matrix C is square. Consequently, for shape functions of the polynomial degree k a number of nodes on the reference element have to be defined, i.e. $K = \frac{1}{2}(k+1)(k+2)$ nodes. This means, the solution of the stated problem leads to a $K \times K$ coefficient matrix C. Exemplary, for $k = 2$ this leads to the coefficient matrix

$$\mathrm{C} = \begin{bmatrix} 1 & 0 & 0 & 0 & 0 & 0 \\ -3 & -1 & 0 & 4 & 0 & 0 \\ -3 & 0 & -1 & 0 & 0 & 4 \\ 2 & 2 & 0 & -4 & 0 & 0 \\ 4 & 0 & 0 & -4 & 4 & -4 \\ 2 & 0 & 2 & 0 & 0 & -4 \end{bmatrix}.$$

Then the i-th quadratic shape function $\psi_i(\xi,\eta)$ is given with

$$\psi_i(\xi,\eta) = c_{1,i} + c_{2,i}\xi + c_{3,i}\eta + c_{4,i}\xi^2 + c_{5,i}\xi\eta + c_{6,i}\eta^2.$$

Analogously, the matrix C can be computed for higher polynomial degrees k.

B.2 Shape Functions of the Argyris Element

The solution of the problem (4.10) leads to a 21×21 coefficient matrix C. Using the employed reference element this leads to

$$
\mathrm{C} = \begin{bmatrix}
0 & 0 & 0 & 1 & 0 & 0 & 0 & 0 & 0 & 0 & 0 & 0 & 0 & 0 & 0 & 0 & 0 & 0 & 0 & 0 & 0 \\
0 & 0 & 0 & 1 & 0 & 0 & 0 & 0 & 0 & 0 & 0 & 0 & 0 & 0 & 0 & 0 & 0 & 0 & 0 & 0 & 0 \\
0 & 0 & 0 & 0 & 1 & 0 & 0 & 0 & 0 & 0 & 0 & 0 & 0 & 0 & 0 & 0 & 0 & 0 & 0 & 0 & 0 \\
0 & 0 & 0 & 0 & 0 & 0 & 0 & 0 & 0 & 0.5 & 0 & 0 & 0 & 0 & 0 & 0 & 0 & 0 & 0 & 0 & 0 \\
0 & 0 & 0 & 0 & 0 & 0 & 0 & 0 & 0 & 0 & 1 & 0 & 0 & 0 & 0 & 0 & 0 & 0 & 0 & 0 & 0 \\
0 & 0 & 0 & 0 & 0 & 0 & 0 & 0 & 0 & 0 & 0 & 0.5 & 0 & 0 & 0 & 0 & 0 & 0 & 0 & 0 & 0 \\
-10 & 10 & 0 & -6 & 0 & -4 & 0 & 0 & 0 & -1.5 & 0 & 0 & 0.5 & 0 & 0 & 0 & 0 & 0 & 0 & 0 & 0 \\
0 & 0 & 0 & 0 & -11 & 0 & -5 & 0 & 0 & 0 & -4 & 0 & 0 & 1 & 0 & 0 & 0 & 0 & 16 & 0 & 0 \\
0 & 0 & 0 & -11 & 0 & 0 & 0 & -5 & 0 & 0 & -4 & 0 & 0 & 0 & 0 & 0 & 1 & 0 & 0 & -16 & 0 \\
-10 & 0 & 10 & 0 & -6 & 0 & 0 & 0 & -4 & 0 & 0 & -1.5 & 0 & 0 & 0 & 0 & 0 & 0.5 & 0 & 0 & 0 \\
15 & -15 & 0 & 8 & 0 & 7 & 0 & 0 & 0 & 1.5 & 0 & 0 & -1 & 0 & 0 & 0 & 0 & 0 & 0 & 0 & 0 \\
0 & 0 & 0 & 0 & 18 & 0 & 14 & 0 & 0 & 0 & 5 & 0 & 0 & -3 & 0 & 0 & 0 & 0 & -32 & 0 & 0 \\
-30 & 15 & 15 & 10 & 10 & -3.5 & 18.5 & 18.5 & -3.5 & -1.5 & 10 & -1.5 & 0.25 & -3.5 & 1.25 & 1.25 & -3.5 & 0.25 & -32 & 32 & $8\sqrt{2}$ \\
0 & 0 & 0 & 18 & 0 & 0 & 0 & 14 & 0 & 0 & 5 & 0 & 0 & 0 & 0 & 0 & -3 & 0 & 0 & 32 & 0 \\
15 & 0 & -15 & 0 & 8 & 0 & 0 & 0 & 7 & 0 & 0 & 1.5 & 0 & 0 & 0 & 0 & 0 & -1 & 0 & 0 & 0 \\
-6 & 6 & 0 & -3 & 0 & -3 & 0 & 0 & 0 & -0.5 & 0 & 0 & 0.5 & 0 & 0 & 0 & 0 & 0 & 0 & 0 & 0 \\
0 & 0 & 0 & 0 & -8 & 0 & -8 & 0 & 0 & 0 & -2 & 0 & 0 & 2 & 0 & 0 & 0 & 0 & 16 & 0 & 0 \\
30 & -15 & -15 & 1 & -10 & 3.5 & -18.5 & -13.5 & 3.5 & 1.5 & -6 & 1 & -0.25 & 3.5 & -0.75 & -1.25 & 2.5 & -0.25 & 32 & -16 & $-8\sqrt{2}$ \\
30 & -15 & -15 & -10 & 1 & 3.5 & -13.5 & -18.5 & 3.5 & 1 & -6 & 1.5 & -0.25 & 2.5 & -1.25 & -0.75 & 3.5 & -0.25 & 16 & -32 & $-8\sqrt{2}$ \\
0 & 0 & 0 & -8 & 0 & 0 & 0 & -8 & 0 & 0 & -2 & 0 & 0 & 0 & 0 & 0 & 2 & 0 & 0 & -16 & 0 \\
-6 & 0 & 6 & 0 & -3 & 0 & 0 & 0 & -3 & 0 & 0 & -0.5 & 0 & 0 & 0 & 0 & 0 & 0.5 & 0 & 0 & 0
\end{bmatrix}.
$$

Then the i-th shape function $\psi_i(\xi,\eta)$ is given with

$$
\begin{aligned}
\psi_i(\xi,\eta) = {} & c_{1,i} + c_{2,i}\xi + c_{3,i}\eta \\
& + c_{4,i}\xi^2 + c_{5,i}\xi\eta + c_{6,i}\eta^2 \\
& + c_{7,i}\xi^3 + c_{8,i}\xi^2\eta + c_{9,i}\xi\eta^2 + c_{10,i}\eta^3 \\
& + c_{11,i}\xi^4 + c_{12,i}\xi^3\eta + c_{13,i}\xi^2\eta^2 + c_{14,i}\xi\eta^3 + c_{15,i}\eta^4 \\
& + c_{16,i}\xi^5 + c_{17,i}\xi^4\eta + c_{18,i}\xi^3\eta^2 + c_{19,i}\xi^2\eta^3 + c_{20,i}\xi\eta^4 + c_{21,i}\eta^5.
\end{aligned}
$$

REFERENCES

[1] ABEDI, R., HAWKER, M. A., HABER, R. B., AND MATOUŠ, K. An adaptive space-time discontinuous Galerkin method for cohesive models of elastodynamic fracture. *International Journal for Numerical Methods in Engineering 81*, 10 (2010), 1207–1241.

[2] AIMI, A., AND DILIGENTI, M. A new space-time energetic formulation for wave propagation analysis in layered media by BEMs. *International Journal for Numerical Methods in Engineering 75*, 9 (2008), 1102–1132.

[3] ALTENBACH, H. *Kontinuumsmechanik: Einführung in die materialunabhängigen und materialabhängigen Gleichungen*. Springer-Verlag, 2015.

[4] ARGYRIS, J. H., FRIED, I., AND SCHARPF, D. W. The TUBA family of plate elements for the matrix displacement method. *The Aeronautical Journal 72*, 692 (1968), 701–709.

[5] ARNOLD, D. N., BREZZI, F., COCKBURN, B., AND MARINI, L. D. Unified analysis of discontinuous Galerkin methods for elliptic problems. *SIAM Journal on Numerical Analysis 39*, 5 (2002), 1749–1779.

[6] BABUŠKA, I. Error-bounds for finite element method. *Numerische Mathematik 16*, 4 (1971), 322–333.

[7] BABUŠKA, I. The finite element method with penalty. *Mathematics of Computation 27*, 122 (1973), 221–228.

[8] BARRETT, J. W., AND ELLIOTT, C. M. Finite element approximation of the Dirichlet problem using the boundary penalty method. *Numerische Mathematik 49*, 4 (1986), 343–366.

[9] BOFFI, D., BREZZI, F., FORTIN, M., ET AL. *Mixed Finite Element Methods and Applications*, vol. 44. Springer, 2013.

[10] BRAESS, D. Finite elements: Theory, fast solvers, and applications in solid mechanics. *Computing in Science & Engineering 1*, 2 (1999), 81–81.

[11] BRENNER, S., AND SCOTT, R. *The Nathematical Theory of Finite Element Methods*, vol. 15. Springer Science & Business Media, 2007.

[12] CHRISTENSEN, R. *Theory of Viscoelasticity: An Introduction*. Elsevier, 2012.

[13] DEMKOWICZ, L., AND GOPALAKRISHNAN, J. A class of discontinuous Petrov–Galerkin methods. part I: The transport equation. *Computer Methods in Applied Mechanics and Engineering 199*, 23-24 (2010), 1558–1572.

[14] DEMKOWICZ, L., AND GOPALAKRISHNAN, J. A class of discontinuous Petrov–Galerkin methods. II. optimal test functions. *Numerical Methods for Partial Differential Equations 27*, 1 (2011), 70–105.

[15] DEMKOWICZ, L., GOPALAKRISHNAN, J., NAGARAJ, S., AND SEPULVEDA, P. A spacetime DPG method for the Schrödinger equation. *SIAM Journal on Numerical Analysis 55*, 4 (2017), 1740–1759.

[16] DEMKOWICZ, L., GOPALAKRISHNAN, J., AND NIEMI, A. H. A class of discontinuous Petrov–Galerkin methods. part III: Adaptivity. *Applied Numerical Mathematics 62*, 4 (2012), 396–427.

[17] DOMÍNGUEZ, V., AND SAYAS, F.-J. Algorithm 884: A simple matlab implementation of the Argyris element. *ACM Transactions on Mathematical Software (TOMS) 35*, 2 (2008), 16.

[18] FELIPPA, C. A. Introduction to finite element methods. *Course Notes, Department of Aerospace Engineeing Sciences, University of Colorado at Boulder, available at http://www. colorado. edu/engineering/Aerospace/CAS/courses. d/IFEM. d* (2004).

[19] FEYNMAN, R. P., LEIGHTON, R. B., AND SANDS, M. *The Feynman Lectures on Physics, Vol. I: The New Millennium Edition: Mainly Mechanics, Radiation, and Heat*, vol. 1. Basic Books, 2011.

[20] GOPALAKRISHNAN, J., AND SEPULVEDA, P. A spacetime DPG method for acoustic waves. *arXiv preprint arXiv:1709.08268* (2017).

[21] HEUSER, H. G. *Functional Analysis, A Wiley-Interscience Publication*. John Wiley & Sons, Ltd., Chichester, 1982.

[22] HUGHES, T. J., AND HULBERT, G. M. Space-time finite element methods for elastodynamics: Formulations and error estimates. *Computer Methods in Applied Mechanics and Engineering 66*, 3 (1988), 339–363.

[23] HULBERT, G. M., AND HUGHES, T. J. Space-time finite element methods for second-order hyperbolic equations. *Computer Methods in Applied Mechanics and Engineering 84*, 3 (1990), 327–348.

[24] JUNG, M., AND LANGER, U. *Methode der finiten Elemente für Ingenieure*. Springer, 2001.

[25] KARKULIK, M., PAVLICEK, D., AND PRAETORIUS, D. On 2D newest vertex bisection: Optimality of mesh-closure and H1-stability of L2-projection. *Constructive Approximation 38*, 2 (2013), 213–234.

[26] KIRBY, R. C., LOGG, A., ROGNES, M. E., AND TERREL, A. R. Common and unusual finite elements. In *Automated Solution of Differential Equations by the Finite Element Method*. Springer, 2012, pp. 95–119.

[27] MARSDEN, J. E., AND HUGHES, T. J. *Mathematical Foundations of Elasticity*. Courier Corporation, 1994.

[28] MIKHLIN, S. G. *Variational Methods in Mathematical Physics*, vol. 50. Pergamon Press;[distributed by Macmillan, New York], 1964.

[29] MORSE, P. M., AND INGARD, K. U. *Theoretical Acoustics*. Princeton university press, 1968.

[30] NEUMÜLLER, M. Space-time methods: Fast solvers and applications, volume 20 of monographic series TU Graz: Computation in engineering and science. *Verlag der TU Graz* (2013).

[31] RUDNICKI, J. W. *Fundamentals of Continuum Mechanics*. John Wiley & Sons, 2014.

[32] SCHEMANN, M., AND BORNEMANN, F. A. An adaptive Rothe method for the wave equation. *Computing and Visualization in Science 1*, 3 (1998), 137–144.

[33] SCHIESSER, W. E. *The Numerical Method of Lines: Integration of Partial Differential Equations*. Elsevier, 2012.

[34] STEINBACH, O. *Numerical Approximation Methods for Elliptic Boundary Value Problems: Finite and Boundary Elements*. Springer Science & Business Media, 2007.

[35] STEINBACH, O. Space-time finite element methods for parabolic problems. *Computational Methods in Applied Mathematics 15*, 4 (2015), 551–566.

[36] STRANG, G., AND FIX, G. J. *An Analysis of the Finite Element Method*, vol. 212. Prentice-hall Englewood Cliffs, NJ, 1973.

[37] YOSIDA, K. *Functional Analysis*. Classics in Mathematics. Springer Berlin Heidelberg, 1995.